



Structural Design and Applications of Stereoregular Fused Thiophenes and Their Oligomers and Polymers

Zexu Xue, Shuai Chen, Nan Gao, Yu Xue, Baoyang Lu, Olivia Anielle Watson, Ling Zang & Jingkun Xu

To cite this article: Zexu Xue, Shuai Chen, Nan Gao, Yu Xue, Baoyang Lu, Olivia Anielle Watson, Ling Zang & Jingkun Xu (2020) Structural Design and Applications of Stereoregular Fused Thiophenes and Their Oligomers and Polymers, Polymer Reviews, 60:2, 318-358, DOI: 10.1080/15583724.2019.1673404

To link to this article: <https://doi.org/10.1080/15583724.2019.1673404>



Published online: 15 Oct 2019.



Submit your article to this journal [↗](#)



Article views: 161



View related articles [↗](#)



View Crossmark data [↗](#)



Citing articles: 5 View citing articles [↗](#)

REVIEW



Structural Design and Applications of Stereoregular Fused Thiophenes and Their Oligomers and Polymers

Zexu Xue^a, Shuai Chen^{a,b}, Nan Gao^a, Yu Xue^a, Baoyang Lu^c, Olivia Anielle Watson^b, Ling Zang^b, and Jingkun Xu^a

^aSchool of Pharmacy, Jiangxi Science & Technology Normal University, Nanchang, China; ^bDepartment of Materials Science and Engineering, Nano Institute of Utah, University of Utah, Salt Lake City, Utah, USA; ^cDepartment of Mechanical Engineering, Massachusetts Institute of Technology, Cambridge, Massachusetts, USA

ABSTRACT






Stereoregular fused thiophenes (SFTs: especially thieno[3,2-*b*]thiophene (TT) and dithieno[3,2-*b*:2',3'-*d*]thiophene (DTT)), as stable conjugated structures deriving from thiophene ring enlargement, possess outstanding properties and special configuration, such as the superior carrier transfer efficiency and a high degree backbone of planarity. In comparison to stand-alone SFTs structures, oligomers and polymers containing different heteroaromatic units have been much widely researched and used in many fields. In decade, several important reviews have summarized the broad field of fused thiophenes including SFTs, and their synthesis and optoelectronic applications. Here, we critically present the structure–performance relationships and application of oligomers and polymers containing SFTs (exhibiting thiophene ring number from 2 to 7) units. First, the basic structures and properties of SFTs are briefly stated. Then, oligomers classified by extra conjugated heterocyclic attachments are carefully discussed, focusing on the structure–performance relationships for their optoelectronic applications including organic photovoltaic cells and organic field-effect transistors. Moreover, such relationships in polymers have been applied in much wider fields such as organic light-emitting diodes, electrochromic devices, thermoelectric devices, and supercapacitors are discussed. Finally, a summary and prospect are given. Through this review, instruction for molecular design and novel ideas for the future development of SFTs-contained are provided.

ARTICLE HISTORY

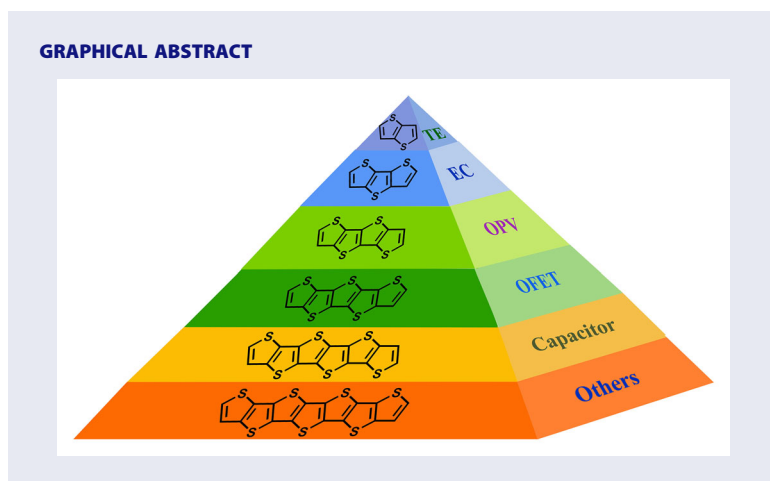
Received 14 March 2019
Accepted 16 September 2019

KEYWORDS

Organic electronics;
aromatic heterocycles;
fused thiophenes;
oligomers; conjugated
polymers

CONTACT Shuai Chen  shuai.chen@utah.edu  School of Pharmacy, Jiangxi Science & Technology Normal University, Nanchang, Jiangxi 330013, China; Ling Zang  lzang@eng.utah.edu  Department of Materials Science and Engineering, Nano Institute of Utah, University of Utah, Salt Lake City, Utah 84112, USA; Jingkun Xu  xujingkun@tsinghua.org.cn  School of Pharmacy, Jiangxi Science & Technology Normal University, Nanchang, Jiangxi 330013, China.

Color versions of one or more of the figures in the article can be found online at www.tandfonline.com/lmsc.



1. Introduction

Advanced electronic applications based on heterocyclic aromatic materials have been emerging in the past several decades owing to their intrinsic organic characters such as tunable structures, good processability, and so on, as well as distinguished multifunctionality and rich electronic performances. Thiophene, as one of the most stable penta-heterocycles, is one of the research focuses on these fields. Its numerous oligomers and polymers (e.g., PThs) have been widely applied in organic photovoltaic cells (OPVs), organic field-effect transistors (OFETs), organic light-emitting diodes (OLEDs), electrochromic devices (ECs), and thermoelectric devices (TEs), etc.^[1–5] Theoretically, the skeleton structures of PThs are configured by single bonds to link adjacent thienyl rings, resulting in poor solubility and molecular planarity. These, significantly confine their electronic applications where high carrier mobilities and facile fabrication technology are preferred. For solubility improvement, various side-chain modification strategies have been proved to be quite effective, however, such functionalization plays a weak role in improving the molecular conjugation and enhancing carrier transport.

To these issues, besides the ordered assembly of polymer chains via non-covalent weak interaction, the most important progress should be the rapid development of fused thiophenes, that is, expanding numbers of conjugated thiophenyl rings along the parallel direction. In the past decade, hundreds of papers along with several important reviews have been published. In 2010, Wu et al.^[2] focused on the active materials mainly composed of fused thiophene rings for OFETs application. In 2015, Cinar and Ozturk^[3] summarized the synthesis methods and fundamental physicochemical properties of oligomers and polymers based on. Later in 2017, Turkoglu et al.^[6] overviewed the applications of thiophenyl-based organic semiconductors covering that having fused thiophene units in OPV, OFET, and OLED fields. Among various fused thiophene structures, stereoregular fused thiophenes (SFTs), including thieno[3,2-*b*]thiophene (TT), dithieno[3,2-*b*:2',3'-*d*]thiophene (DTT), tetrathienoacene (TTA), pentathienoacene (PTA), hexathienoacene (HTA), and heptathienoacene (HPTA), possess specific advantages such as high planar conformation, good conjugated architectures, adjustable

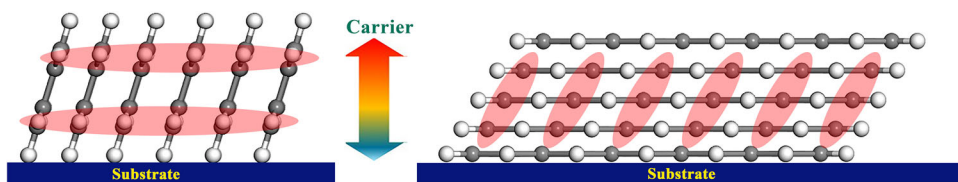


Figure 1. Two stacking conformations, edge-on (left) and face-on (right), of SFTs on substrate surfaces. The direction of carrier transfer is vertical with substrate.

energy levels, excellent environment stability, and so on, due to their flat and conjugated skeletons and rigid geometric constructions.^[3,7–9] Meanwhile, their electron-rich structures that possess sulfur atoms are favorable to elevate the crystallization of their oligomers and polymers by intermolecular interaction. The crystallization is proved to be quite beneficial to achieve high carrier mobility in molecular system and extend device lifetime.^[6,10–13]

Moreover, in contrast to pentacene which has been demonstrated as a promising aromatic material for high-efficiency organic thin film transistors (OTFTs), SFTs inherit the facile functionalization of PThs through attaching flexible alkyl chains, electron-withdrawing or electron-donating substituents at flanking positions. Thus, their (homo- or co-) oligomers and polymers are with much-enhanced solubility and better performances for opto-/electronic- or other applications. In particular, the incorporation of side groups does not necessarily mean the loss of molecular ordering in view of macromolecular arranging regularity through the intermolecular stacking of rigid backbones of SFTs, although sometimes researches have to keep a balance between the solubility and charge carrier mobility when long chains are incorporated into the molecular skeletons.^[14–16] Overall, SFTs-contained oligomers and polymers have been extensively researched in optoelectronic fields, mainly focusing on increasing the device efficiency via elaborate molecular design in line with controlled conformations and selective fabrication methods. In addition, according to X-ray diffraction (XRD) characterization, two general molecular π - π stacking patterns of SFTs molecules, ‘edge-on’ and ‘face-on’ (Figure 1) on substrate surfaces, could appear. They are favorable to augment carrier transport in full device system due to the formation of one-dimensional transmission line at molecule to molecule and substrate to molecule. Similarly, regular aggregates of PTCDis with enhanced carrier mobility compared to normal monomer molecules have been researched and discussed in our previous papers.^[17–23] SFTs and their oligomers and polymers have earned a significant space in active materials for organic electronics. Besides to widely use in OPVs, etc., our group and others have also paid attention to SFTs-based ECs and TEs.^[24–26]

Thus, in this review, we devote to summarize the advances and compare the structural characteristics and applied performances of SFTs as well as their oligomers and polymers, especially in the past five years. For oligomers, the logic organization is presented according to various skeleton units aligned with SFTs, while the representation for polymers is following their application fields due to their quite complex structures. Special attention is paid to discussing the relationship between molecular structures and electronic properties accompanying applications. At last, the cautious evaluations of current challenges and prospect on this field are stated.

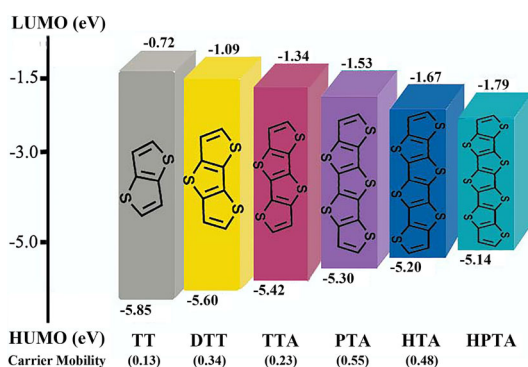


Figure 2. DFT-derived SFTs orbitals data and carrier mobility from TT to HPTA.

2. Stereoregular fused thiophenes (SFTs)

Till now, the reported basic structures of SFTs contain TT, DTT, TTA, PTA, HTA, and HPTA, in response to the number of thiophene rings from 2 to 7, respectively. They all have intrinsically planar conjugated structures and active substitutional sites, enabling further functionalization to achieve more structural and performance superiority. As the backbones enlarge from TT to HPTA, the molecular rigid planarity, conjugation degree, and thermal stability gradually increase. Meanwhile, these SFTs exhibit successively smaller band gaps (Figure 2) and thus diverse optical, electronic, and electrochemical properties. Further, all the sulfur atoms are positioned at the molecular periphery, facilitating multiple short intermolecular S...S contacts, which will increase the effective dimensionality of the electronic structures to allow for enhanced transport properties.^[27–29] According to density functional theory (DFT) calculations and real transistor devices based on SFTs, PTA displays the highest carrier mobility, with hole mobility of $0.55 \text{ cm}^2 \text{ V}^{-1} \text{ S}^{-1}$ and electron mobility of $0.80 \text{ cm}^2 \text{ V}^{-1} \text{ S}^{-1}$. However, HTA, since it shows a bit smaller data (0.48 and $0.22 \text{ cm}^2 \text{ V}^{-1} \text{ S}^{-1}$ for the hole and electron mobility, respectively) due to the longer carrier transfer distance in the whole molecule. Circularly-fused thiophenes present extreme loss of conjugation and increased symmetry leading to poor optical absorption in the visible or near-UV range.^[27,30]

Nevertheless, single molecular SFTs as the active material can't achieve satisfactory application performances owing to its rigid structure, limited conjugation, molecular defect, etc. On account of their poor solubility in organic solvents, material processable technology is another serious problem to realize the practical application. For these reasons, SFTs are usually employed as important skeleton cores or π -bridge between donor (D) and acceptor (A) units in optoelectronic fields to elevate carrier mobilities strengthen optical absorption enhance π - π stacking ability, and others.^[10,31–33] Also, modification by side-chains (e.g., alkyl chains) has been widely used. Generally, oligomers and polymers containing SFTs and functional groups with D-A, D- π -A, or D- π -D constructions are much more widely applied in optoelectronic devices.^[31,34,35]

3. Oligomers and applications

Oligomers containing SFTs units can significantly enlarge their applications by compositing with other D- or A-type groups, including but not limited to typical

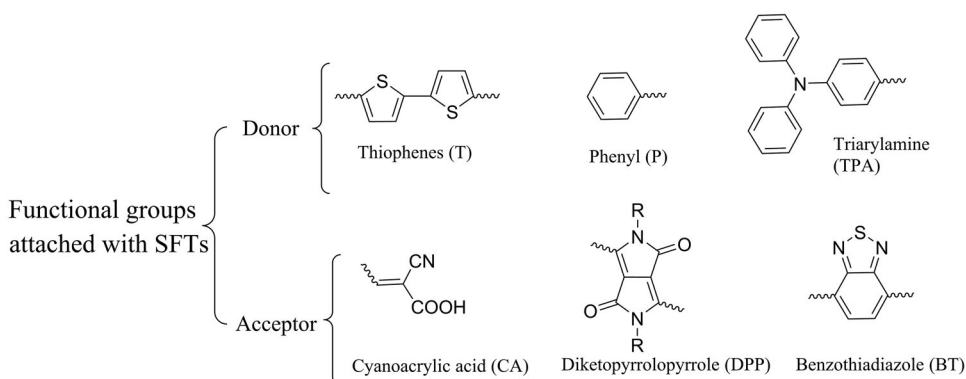


Figure 3. Typical functional units (donor and acceptor) attached with SFTs units.

examples in [Figure 3](#) and their derivatives. For D-type groups, they usually possess a high degree of conjugated planarity, making the whole molecule have very good planarity. For A-type groups, they exhibit strong electron-withdrawing ability, facile synthesis good solubility, strong light absorption, etc.^[11,32,36,37] The main purposes of these design are to gain excellent carrier mobility and promising processibility for desired application of oligomers in OPVs and OFETs devices.^[38]

OFETs as logical devices exhibit four basic device constructions ([Figure 4](#)). SFTs are usually appeared as active semiconductor materials in the bottom-gate top-contact type.^[2,39] In general, high performances for transistors means high carrier mobility (μ), large on/off ratio ($I_{\text{on}}/I_{\text{off}}$) value, and low threshold voltage (V_T), as well as good material stability, where molecular SFTs possess limits as mentioned above.

OPVs as the most important solar-induced electronic power generation devices also have different configuration ([Figure 4](#)), and in addition to stability, are evaluated by high power conversion efficiency (PCE) to represent their high performances. It can be measured according to the following formula:

$$\text{FF} = \frac{I_m V_m}{V_{oc} J_{sc}} \quad (1)$$

$$\text{PCE} = \text{FF} \frac{J_{sc} V_{oc}}{P_{in}} \quad (2)$$

where I_m is the maxima current power points, V_m is the maxima voltage power points. J_{sc} is the short circuit current, V_{oc} is the open-circuit voltage, FF is the fill factor, and P_{in} is the incident light power density.^[40] SFTs-based oligomers are mainly employed as active material on bulk heterojunction solar cell (BHJ), as shown in [Figure 4](#).^[40,41]

3.1. Attaching thiophenyl units

Thiophene possesses the aromatic five-membered with a high molecular resonance energy (29 kcal mol^{-1}).^[9] In SFTs-contained oligomers, thienyl units are usually located at the α -position of SFTs unit, which acted as π -bridge linking or end-capping group. Through controlling horizontal order of oligomer molecules, highly planar and rigid thienyl units can enhance their π - π overlap in the solid state, and thus lead to efficient

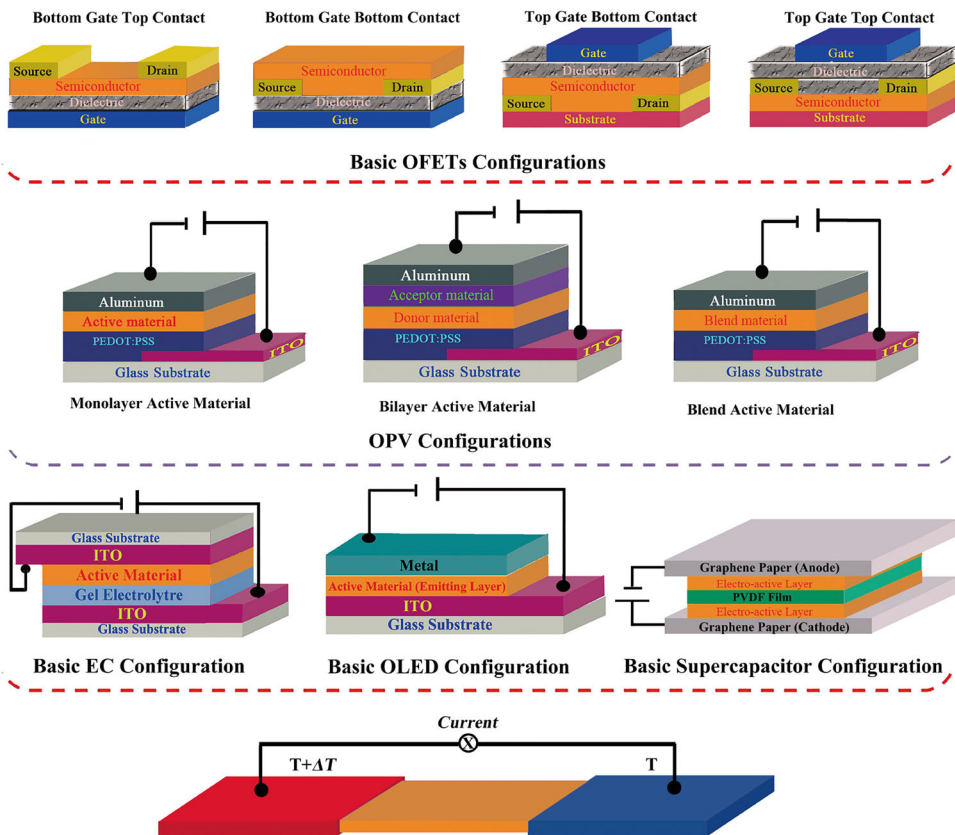


Figure 4. Basic opto-/electronic devices configurations based on organic active materials containing SFTs structures.

intra-/inter-molecular charge transport, resulting into high carrier mobilities mainly in OFETs.^[2] The decoration of terminal thienyl rings also can reduce their steric hindrance and facilitate solution-processability.^[42] A summary of reported molecular structures attaching thienyl units, their optical and electrochemical properties, and application performances as OFETs devices is shown in Figure 4 and Tables 1 and 2, respectively. When the effective conjugated lengths of molecular skeleton increase, the maximum absorption peaks (λ_{abs}^{max}) of these oligomers exhibit red-shift and the optical band gaps (E_g^{opt}) decrease.

For the effect of SFTs-based active materials on OFETs performances, it can be seen that under possessing same number thiophenyl rings to TT cores in oligomers 1–5, alkyl chain modification at horizontal direction has a little effect.^[43–45] However, when alkyl chains are introduced at the side face of molecular skeletons, the steric hindrance increases leading to bigger between neighboring molecules and thus degrading the device performances. Indeed, although symmetrical oligomer 9 possesses an extended conjugated structure, oligomer 6 reveals much greater performances owing to its very planar molecular structure.^[44,46] However, oligomer 15 (Figure 5), which possesses two planar DTT molecules, has a special π -stacked structure. It is profitable for electronic migration on solid state due to face-to-face molecular stacking.^[47] Similar behavior of

Table 1. Optical and electrochemical properties of SFTs-contained oligomers having thienyl units.

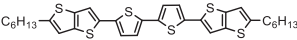
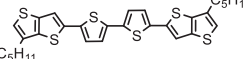
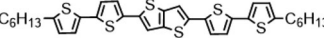
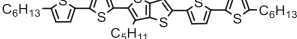
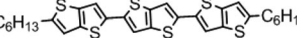
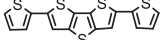
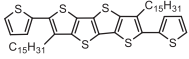
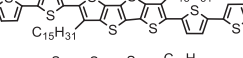
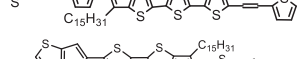
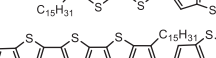
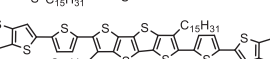

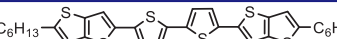
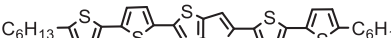
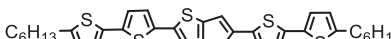
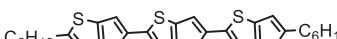

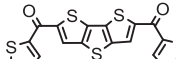
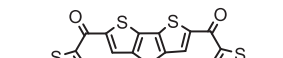
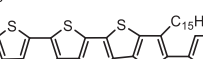
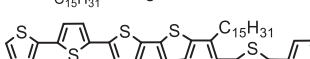
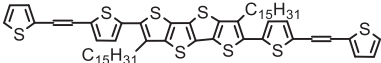
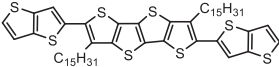
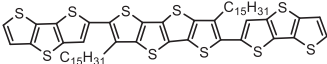
Oligomer	Structure	λ_{abs}^{max}/nm	E_{ox}^{onset}/V	HOMO/eV	LUMO/eV	E_g^{opt}/eV
1		417	0.83	-5.27	-2.75	2.51
2		396	0.64	-5.08	-2.52	2.62
3		433	0.75	-5.19	-2.71	2.44
4		411	0.72	-5.16	-2.58	2.59
5		359	0.82	-5.26	-2.66	2.67
6		387	0.98	-5.48	-	-
9		390	1.05	-5.25	-2.52	2.73
10		421	0.95	-5.15	-2.63	2.52
11		447	0.89	-5.09	-2.73	2.36
12		409	1.01	-5.21	-2.77	2.44
13		427	0.94	-5.14	-2.90	2.24
14		409	1.01	-5.21	-2.61	2.60

Table 2. Performances of OFETs devices of based on SFTs-contained oligomers.

Oligomer	Structure	$\mu/cm^{-2}V^{-1}S^{-1}$	V_T/V	I_{on}/I_{off} ratio
1		3.1×10^{-3}	-5.5	2.6×10^2
3 ^a		1.1×10^{-2}	-4.2	1.2×10^3
3 ^b		2.5×10^{-2}	-4.0	1.2×10^3
5		0.14	3.6	10^4
6		3.0×10^{-2}	-25	10^4-10^5
7		5.4×10^{-2}	-28.5	10^6-10^7
8		0.18	-18.3	10^4-10^6
9		1.6×10^{-3}	-36	3.1×10^2
10		0.12	-15	10^4-10^5

(continued)

Table 2. Continued.

Oligomer	Structure	$\mu/\text{cm}^{-2}\text{V}^{-1}\text{S}^{-1}$	V_T/V	$I_{\text{on}}/I_{\text{off}}$ ratio
11		0.81	-10	10^3-10^4
12		7.3×10^{-2}	-25.1	10^5-10^6
13		5×10^{-2}	-	10^8

^aThe vacuum deposition of oligomer on substrates at 25 °C. ^bThe vacuum deposition of oligomer on substrates at 70 °C.

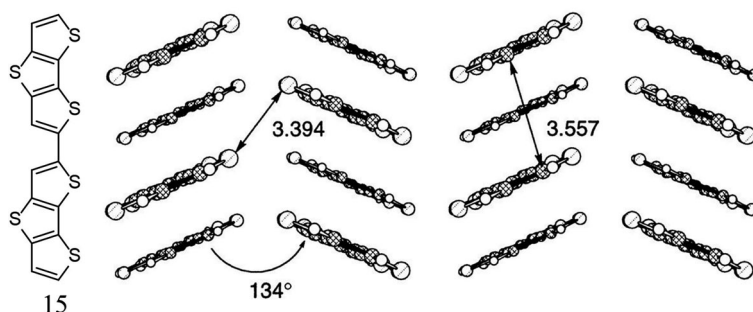


Figure 5. Molecular structures and packing view of oligomer 15. Reprinted with permission from Li et al.^[47] Copyright 1998 American Chemistry Society.

H-type aggregation of oligomer 11 results into enhanced OFETs performances.^[48-50] In addition, it also should be pointed out that same oligomer exhibited different performances under the same fabricated conditions and technology.

When the same or another SFTs units instead thiophenyl groups are introduced into skeleton. Oligomer 12 displays much higher mobility, at least fourfold, than that of oligomer 9. In addition, all mobility data indicate that the increased molecular conjugation length may enhance OFETs performance, mainly by increasing carrier mobilities.

3.2. Attaching arylphenyl units

Generally, arylphenyl units such as phenyl, naphthyl, pyrenyl, xenyl, and their derivatives are located on the terminal position of SFTs-cored oligomers (Figure 6 and Tables 3 and 4) to enhance the stability of materials and devices via retarding oxidation.^[51-57] The incorporation of the phenyl groups can also extend the conjugation of oligomer chromophores, leading to shift of the absorption wavelengths and fluorescence emission, as well as improvement of the fluorescence quantum yields.^[51,58,59] And, just like above-mentioned molecular assembly of planar oligomers, with the increase of phenyl rings (e.g., pyrenyl) to form a more planar structure, one-dimensional nanofibers can be formed which are much beneficial to improve the carrier mobility.^[59-61] In contrast to thiophenyl involved oligomers, much rich variant structures of arylphenyl groups and the diverse carbon-carbon bonds linking them with SFTs units have shown much complex effect on their applied performances in OFETs

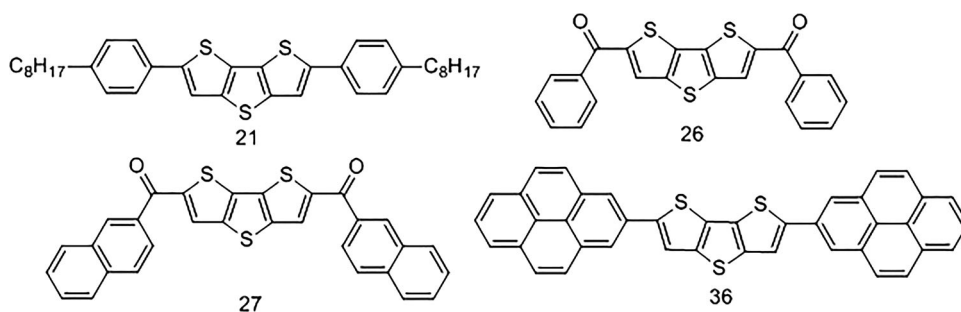
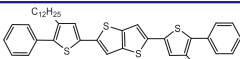
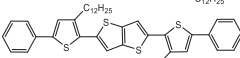
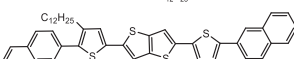
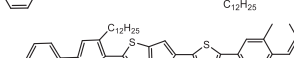
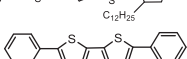
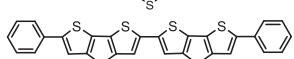
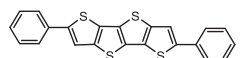
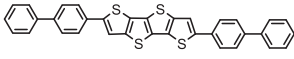
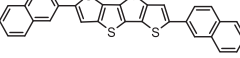
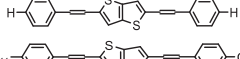
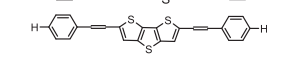
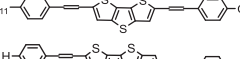
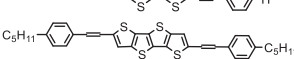
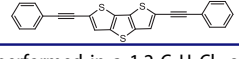

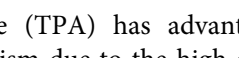


Figure 6. Molecular structures of oligomers 21, 26, 27, and 36 with DTT as center group with symmetrical bis-aryl terminal units.

and other devices. As seen from Table 3, the linking way and the number of arylphenyl are intimately involved in molecular structure although often implicitly ignored in designing molecules. The presence of double or triple bonds in these oligomers can facilitate π -electron delocalization among the whole molecular skeleton, and effectively extend the conjugation length of the system. Moreover, although it is the attachment of side groups like alkyl chains that maintain the molecular solubility, they will bring some negligible effect on the device performances. For example, some specific molecules (e.g., PTCDis) attaching alkyl chains usually indistinguishable absorption and emission properties which reduce PCE efficiency of OPVs devices.^[62]

In line with the molecular structures, as listed in Table 4, the fabrication conditions such as deposited temperatures of layers of these oligomers also play significant roles on the OFETs device performances. On one hand, under the same fabrication technology, oligomer 31 exhibiting a greater conjugated naphthyl shows improved performance than that of oligomer 30 having end-capped biphenyls.^[55] On the other hand, treated temperatures can affect crystalline state of oligomer layers and the optimal conditions also depend on the planarity of molecular structures which means shorter distances of molecular stacking, such as oligomer 23. Besides active materials themselves, their interfacial contact with substrate is also very critical to achieve effective charge transfer. Often, the small charge injection areas and poor ordering of the organic semiconductor has been experimentally investigated to limit device performance on the electrodes in the bottom-contact geometry. Noteworthy, the performances of OFETs devices based on coating oligomers 20 and 28 octadecyltrichlorosilane (OTS) pre-modified substrates can be improved in contrast to that with untreated substrates. For this, the reduced interfacial energy between the oligomer and the substrate having previously self-assembled OTS monolayer is the key factor.^[63–65] In short, the device performances should match well with the oligomers, their film microstructures, and surfaces morphology of both substrate and active material layer. A symmetrical oligomer 36 employing pyrenyl as end-capped group to DTT core was researched as D-type active material for fabricating planar heterojunction devices due to the more conjugated degree of oligomer 36.^[66] Under simulated AM 1.5 solar irradiation at 100 mW cm^{-2} , the device was estimated with PCE of 0.52%, FF of 0.22, J_{SC} of 3.15 mA cm^{-2} , and V_{OC} of 0.76 V. When blended with A-type C_{70} , the PCE value of device can reach 3.60%, due to efficient dissociation of excitons and carrier transport.

Table 3. The optical and electrochemical properties of SFTs-contained oligomers with aryl terminal units.

Oligomer	Structure	$\lambda_{abs}^{max}/\text{nm}$	E_{ox}^{onset}/V	HOMO/eV	LUMO/eV	E_g^{opt}/eV
16		389	–	–5.25	–2.54	2.71
17		401	–	–5.28	–2.55	2.73
18		409	–	–5.20	–2.61	2.66
19		407	–	–5.21	–2.54	2.67
20 ^a		374	1.21	–5.41	–	2.59
28 ^a		431	–	–	–	2.60
29 ^b		383	1.03	–5.43	–	2.67
30 ^b		372	1.01	–5.41	–	2.52
31 ^b		356	0.99	–5.39	–	2.36
32 ^a		–	1.03	–5.43	–	2.53
32 ^b		–	0.73	–5.13	–	2.52
33 ^a		–	0.99	–5.39	–	2.40
33 ^b		–	0.82	–5.22	–	2.58
34 ^a		–	0.96	–5.36	–	2.37
34 ^b		–	0.74	–5.14	–	2.41
35		–	–	–5.54	–	2.95

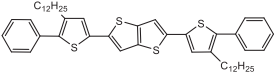
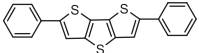
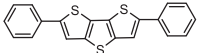
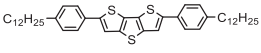
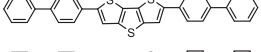
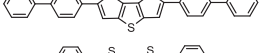
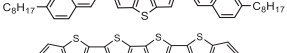
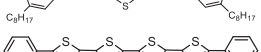
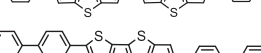
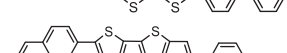
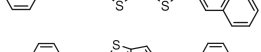
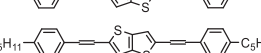
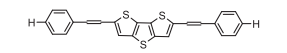
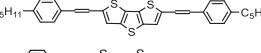
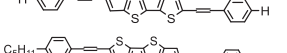
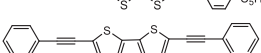
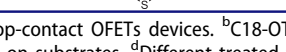
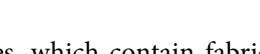
^aMeasurements performed in a 1,2-C₆H₄Cl₂ solution. ^bMeasurements performed in a dilute THF solution.

3.3. Attaching triarylamine and cyanoacrylic acid units

Triarylamine (TPA) has advantages such as good redox activity, fluorescence, and ferromagnetism due to the high oxidizability of the nitrogen center.^[1] It has been noted as one of the most frequently used hole transporting unit to build small D-A type oligomer for OPVs.^[1,67,68] On the contrary, cyanoacrylic acid (CA) usually is adopted as an electron pull in the photosensitizer of dye-sensitized solar cell (DSSC).^[68,69] From Figure 7 and Table 5, the introduction of TPA and CA into SFTs-contained oligomers could increase the λ_{abs}^{max} and HOMO value for 57. Regardless of these two functional groups, different sized alkyl chains located on the same core unit can have some influence on HOMO/LUMO energy level in that alkyl chain could produce steric hindrance that is limited electron transfer.^[31,32,70–76]

Benefiting from the improved electron delocalization via attaching TPA and/or CA units into this series of oligomers, they are mostly used as sensitizer materials in DSSC to lift PCE values. As shown in Table 6, many factors could affect photovoltaic

Table 4. Performances of OFETs devices based on SFTs-contained oligomers with phenyl as terminal units under different treated temperatures.

Oligomer	Structure	Temperature/°C	$\mu/\text{cm}^{-2}\text{V}^{-1}\text{S}^{-1}$	V_{T}/V	$I_{\text{on}}/I_{\text{off}}$ ratio
16		–	3.1×10^{-2}	–	4.5×10^4
20 ^b		25	0.20	–20	1.4×10^5
20 ^c		70	0.42	–23.4	5×10^6
22		–	1.81	–26	10^5
23 ^c		70	0.12	–20.2	5×10^5
23 ^d		120	0.14	–19	10^6
24		–	0.54	–14	10^6
25		–	5.0×10^{-2}	–31	10^5
28 ^b		25	2.6×10^{-2}	–7.3	5.5×10^{-2}
30 ^d		120	5.0×10^{-2}	–31	10^5
31 ^d		120	9.0×10^{-2}	–28	10^6
32 ^a		100	4.0×10^{-2}	–11.5	10^5
32 ^b		100	4.0×10^{-2}	0.8	10^6
33 ^a		70	0.17	–10.1	10^5
33 ^b		70	1.3×10^{-2}	–6.4	2.0×10^{-4}
34 ^a		100	1.4×10^{-2}	–3.5	10^4
34 ^b		70	1.7×10^{-2}	–17.8	10^5
35		–	0.19	–23	1.6×10^7

^aThe data of top-contact OFETs devices. ^bC18-OTS, C8-OTS, BTS, and bare-treated substrates at 25 °C. ^cDifferent treated temperatures on substrates. ^dDifferent treated temperatures and methods.

performances, which contain fabrication technology, the position of alkyl chains and so on.^[70–76] For these devices fabrication, solution-processibility of oligomers is necessary. In most cases, such capability is achieved by attaching branched alkyl chains on the molecule skeleton. Also, alkyl chains can show some effect on the device performances. For example, the device performance based on oligomer 49 is better than 50 and 51, which is determined from the branched alkyl chains substituted in the molecule skeleton to decrease electron transform efficiency. The linear C₁₅-alkyl chain substituent not only prevents oligomer aggregation but also inhibits charge recombination from D to A. Moreover, for most OPVs devices, device stability is an essential parameter to evaluate OPVs devices. The device based on oligomer 41 maintained nearly the

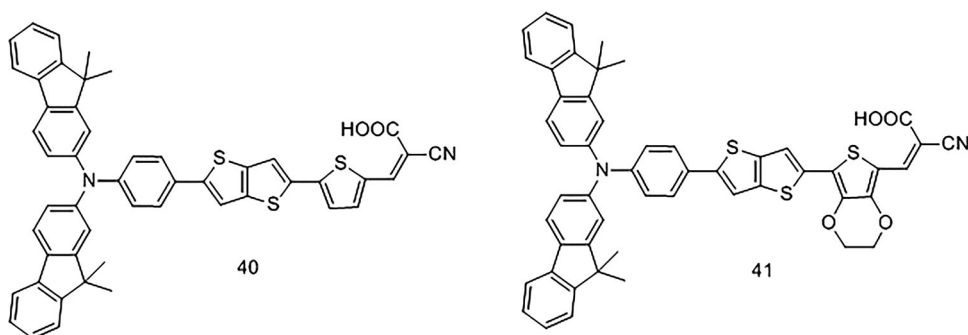


Figure 7. Molecular structures of oligomers 40 and 41.

initial performance values over a period of 45 days. Moreover, for oligomer 48, the incorporation of thiazole unit as a rich-electron linker instead of thiophenyl between TT units results into higher V_{OC} , J_{SC} , and PCE values. These are the performance metrics reported to date for DSSC devices using fused-thiophenes as dye sensitizers, and approach the record PCE of 10.65% for metal-free organic sensitizers recently reported by Yang et al.^[77] using Co (II/III) redox shuttle.

3.4. Attaching diketopyrrolopyrrole units

Diketopyrrolopyrrole (DPP) unit has well-conjugated structures with strong π - π interaction and electron-withdrawing effect, and relatively low lying HOMO and LUMO levels. When embedding them into hybrid conjugated oligomers, it often brings broad and tunable optical absorption, and high mobilities for holes and electrons, which can result in efficient charge transport, high photocurrents and good FF for OPVs and OFETs.^[78–81] As structures are shown in Table 7, DPP units in SFTs-contained oligomers are generally as central or terminal units of molecular backbones forming symmetrical structures.^[82,83]

According to the optical and electrochemical properties of these oligomers listed in Table 7, the presence of DPP units in molecular backbone could obviously decrease E_g^{opt} and the initial oxidation potential (E_{ox}^{onset}), favoring the carrier hopping. For example, oligomer 60 possesses much promising performances of μ than oligomer 9. However, after the insertion of thiophenyl and bithiophenyl between TTA spacer and DPP caps in oligomers 60–65, their λ_{abs}^{max} become blue-shifted. On the contrary, the incorporation of thiophenyl and bithiophenyl at the DPP units results in red-shifted λ_{abs}^{max} .

As summarized in Table 8, the trend of μ values of OFETs fabricated from oligomers 60–65 is following an order of $60 > 62 > 65 > 64 > 61 > 63$. On one side, the long insulating branch side chains leads to a considerable difference in the hole mobility, although they have same HOMO/LUMO energy levels.

For the OPVs devices using oligomers 60–65 as D-type material, PC₇₁BM as the A-type material and 1,8-diiodooctane (DIO) as a solvent additive, as listed in Table 9, the PCE of that based on oligomer 60 achieved the highest value of 4.02%. When the amount of DIO was 1.0 vol%, it achieved the higher PCE which was attributed to a significant increase in J_{SC} . A similar trend was observed for oligomer 65, which was mainly attributed to the higher FF value.

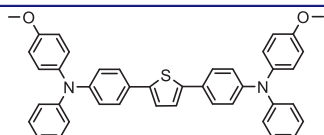
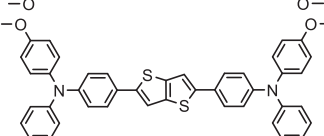
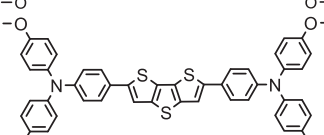
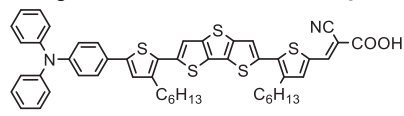
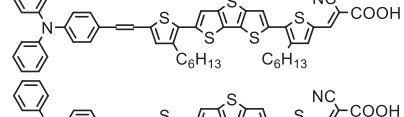
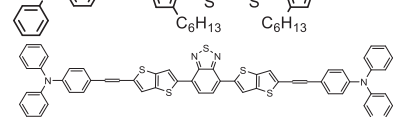
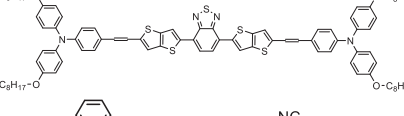
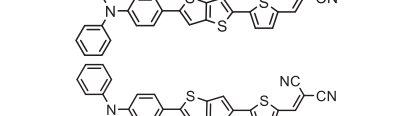
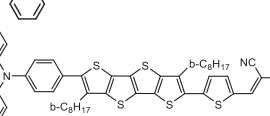
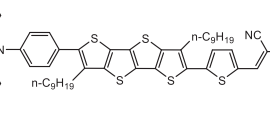
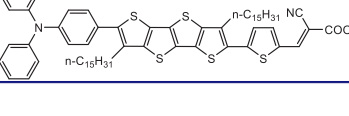


Table 5. Optical and electrochemical properties of SFTs-contained oligomers attached with TPA and/or CA groups.

Oligomer	Structure	λ_{abs}^{max}/nm	E_{ox}^{onset}/V	HOMO/eV	LUMO/eV	E_g^{opt}/eV
37		400	–	–5.25	–2.47	2.78
38		410	–	–5.26	–2.52	2.74
39		420	–	–5.27	–2.59	2.68
45		414	0.39	–5.10	–3.42	1.64
46		420	0.30	–5.01	–3.36	1.61
49		485	0.99	–5.19	–3.27	–
50		498	0.99	–5.19	–3.28	–
51		519	1.00	–5.20	–3.29	–
52		510	–	–5.09	–	1.79
53		500	–	–5.01	–	1.84
54		498	–	–5.29	–3.11	2.18
55		490	–	–5.06	–3.14	2.08
56		482	–	–5.16	–3.08	2.08
57		513	–	–4.95	–3.05	2.04

3.5. Attaching other heterocyclic units

Up to now, most optoelectronic semiconductor materials including the aforementioned SFTs-contained oligomers have shown p-type characteristic, which possesses limitations on devices lifetime, stability, etc. To improve these, n-type semiconductors usually possessing fluorine-contained heterocyclic ring or perylene imide units have been widely applied.^[54,58,84–87]

Table 6. Photovoltaic performances of SFTs-contained oligomers having TPA and/or CA units.

Oligomer	Structure	V_{oc}/V	$J_{sc}/(mA\ cm^{-2})$	FF	PCE/%
37		0.79	11.1	0.49	4.31
38		0.89	15.4	0.60	8.23
39		0.99	17.1	0.67	11.29
42		0.75	14.2	0.72	7.60
43		0.65	13.3	0.73	6.40
44		0.73	15.4	0.75	8.40
45		0.74	5.7	0.34	1.44
46		0.61	3.6	0.34	0.75
47		0.87	11.04	0.57	5.41
48		0.95	12.01	0.54	6.20
49		0.81	17.5	0.72	10.21
50		0.78	15.5	0.62	7.60
51		0.78	16.9	0.69	9.02

(continued)

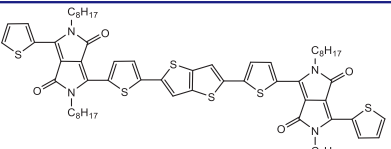
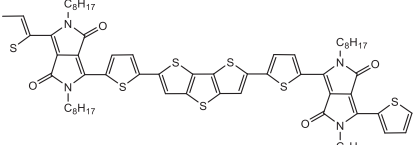
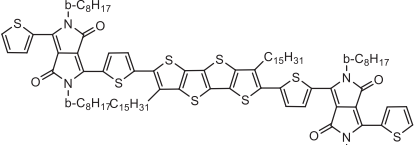
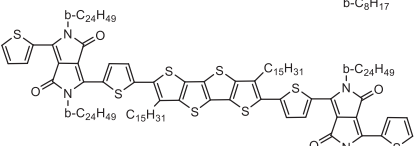
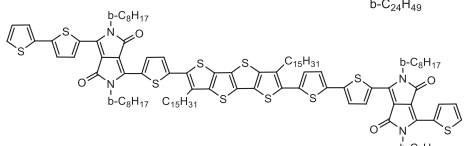
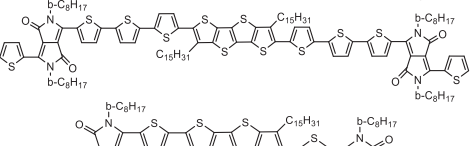
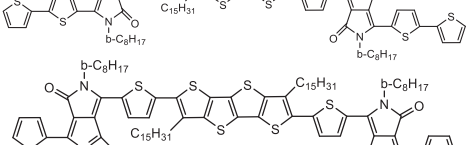
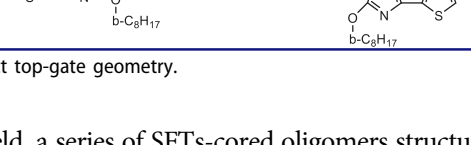
Table 6. Continued.

Oligomer	Structure	V_{oc}/V	$J_{sc}/(\text{mA cm}^{-2})$	FF	PCE/%
52		0.63	1.2	0.42	0.32
53		0.62	-0.98	0.43	0.26
54		0.95	7.7	0.66	4.76
55		0.83	16.3	0.74	10.11
56		0.89	10.1	0.68	6.15
57		0.83	11.8	0.70	6.91

Table 7. Optical and electrochemical properties of SFTs-contained oligomers having DPP units.

Oligomer	Structure	$\lambda_{abs}^{max}/\text{nm}$	E_{ox}^{onset}/V	HOMO/eV	LUMO/eV	E_g^{opt}/eV
58		510	-	-5.12	-3.29	1.61
59		540	-	-5.08	-3.27	1.61
60		615	0.92	-5.12	-3.43	1.69
61		615	0.92	-5.12	-3.43	1.69
62		610	0.88	-5.08	-3.29	1.79
63		608	0.86	-5.06	-3.24	1.82
64		664	0.83	-5.03	-3.37	1.55
65		643	-	-5.06	-3.28	1.66

Table 8. Performances of OFETs devices based on oligomers 58–65 attached with long alkyl side chains.

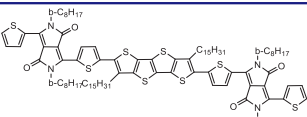
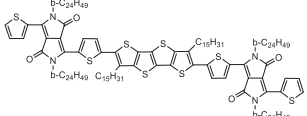
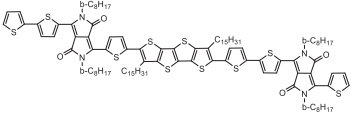
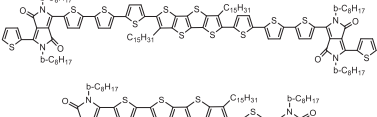
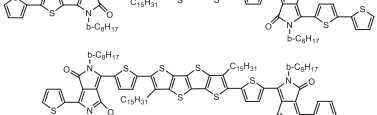
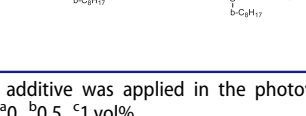
Oligomer	Structure	$\mu/\text{cm}^{-2}\text{V}^{-1}\text{s}^{-1}$	$V_{T/N}$	$I_{\text{on}}/I_{\text{off}}$ ratio
58		4.63×10^{-2}	1.27	3.82×10^6
59		2.19×10^{-2}	-0.61	3.96×10^6
60		0.1	-13.1	2.50×10^4
61		9.4×10^{-3}	-9.2	6.90×10^3
62		2.0×10^{-2}	-14.1	7.40×10^5
63		4.5×10^{-5}	-4.8	2.30×10^3
64		1.3×10^{-2}	-9.6	4.30×10^4
65 ^a		1.8×10^{-2}	-15.6	10^3

^aBottom-contact top-gate geometry.

In this field, a series of SFTs-cored oligomers structures end-capped with pentafluorobenzyl have been reported as shown in Table 10. The optical absorbance spectra of F-substituted molecules in $\text{C}_6\text{H}_4\text{Cl}_2$ solutions nearly overlap with those without F substitution, which could be attributed to the fact that fluoroaryl substitution could lower both the HOMO and LUMO energy. The insertion of pentafluorobenzen in SFTs leads to much blue-shifted $\lambda_{\text{abs}}^{\text{max}}$ and increased E_g^{opt} and $E_{\text{ox}}^{\text{onset}}$ for oligomer 73 than that of 6, and for oligomer 68 than that of 20.

For oligomers 66 and 67, the absorption peaks are slightly red-shifted for that containing the greater number of F atoms. In addition, the E_g^{opt} of oligomers is

Table 9. Photovoltaic performances of oligomers 60–65 when D/A units are blended in different ratios.

Oligomer	Structure	Blend ratio	V_{OC}/V	$J_{SC}/(\text{mA cm}^{-2})$	FF	PCE/%
60		2:3	0.70	7.7	0.50	2.9
61		1:1	0.76	1.8	0.58	0.9
62		2:3	0.70	5.1	0.51	2.0
63		1:1	0.63	3.6	0.39	1.2
64		2:3	0.60	1.5	0.60	0.6
65		–	0.75 ^a	1.9	0.41	0.59
		–	0.73 ^b	7.3	0.40	2.13
		–	0.72 ^c	10.4	0.54	4.02
		–	0.52 ^a	2.1	0.33	0.36
		–	0.60 ^b	1.7	0.48	0.48
		–	0.60 ^c	1.6	0.51	0.38

DIO as a solvent additive was applied in the photovoltaic devices when oligomer 65 is D-type material. The ratio of additive DIO is ^a0, ^b0.5, ^c1 vol%.

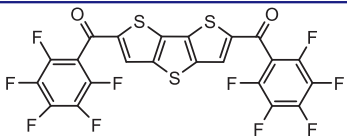
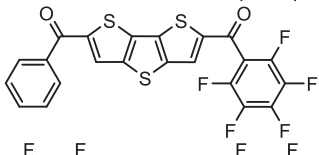
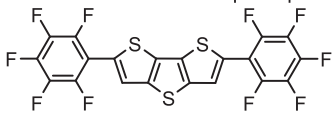
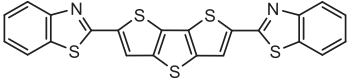
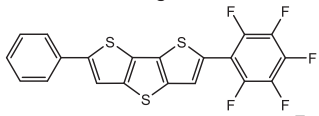
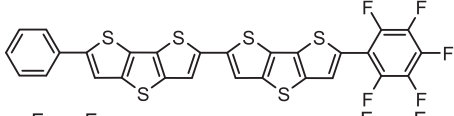
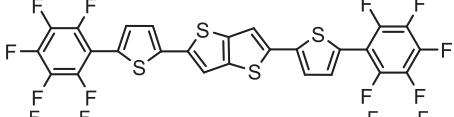
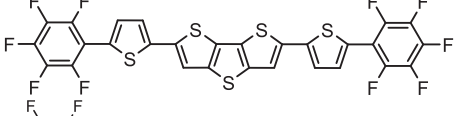
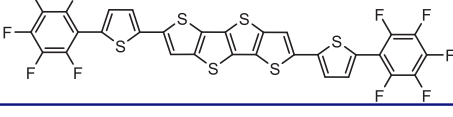
increased in an order of $74 < 73 < 72$. This result indicates that electrons are much delocalized as the size of the SFTs core increases and as additional thienyl units are combined to the fused molecular core.

The F-substituted oligomers generally provide n-channel transport for OFETs. As shown in Table 10, devices based on these oligomers have high E_g^{opt} but low μ . Therefore, how to improve carrier mobility of n-type oligomer is the foremost research focus. Oligomer 74 exhibits a quite similar herringbone packing motif with a dihedral angle of 12° . The shortest interplanar distance between TTA cores is 3.57 \AA and the shortest S–S distance is 3.50 \AA .^[88] The increased degree of π – π overlap in cofacial packing structures can promote much efficient charge transport versus herringbone packing structures.^[89–91]

4. Polymers and applications

Compared with oligomers, SFTs-contained polymers have conjugated structural chains for long-range charge transfer and more abundant reactive sites for attaching functional groups. The stacking of neighboring feasible side-chains and reconstitution of molecular architectures can provide additional chances to enhance material properties and device performances. These polymers with other types of functional materials can lead to much abundant optic and electronic characteristics to meet wide applications.^[92–94]

Table 10. Performances of OFETs devices based on oligomers 66–74 with pentafluorobenzene as end-capped units.

Oligomer	Structure	$\mu/\text{cm}^{-2}\text{V}^{-1}\text{S}^{-1}$	V_{T}/V	$I_{\text{on}}/I_{\text{off}}$ ratio
66		3×10^{-5}	74	10^4
67		4×10^{-6}	-60	10^4
68		3×10^{-4}	74	10^5
69		5×10^{-6}	-17	10^5
70		0.15	-59	8.3×10^6
71		2×10^{-3}	-2	2.3×10^4
72		6×10^{-2}	50	2.9×10^3
73		4.6×10^{-3}	85	3.4×10^5
74		9.9×10^{-4}	73	8.6×10^4

In this section, their applications in OPVs, and OFETs (including OTFTs), ECs, OLEDs, TEs, and supercapacitors (Figure 4) are summarized, and special attention is paid on discussing the relationship between structures and device performances. Fabrication technologies from relative oligomers to polymers, especially electrochemical polymerization and chemical reaction, also have been introduced and their applicability to achieve high-performance materials or devices is discussed.

4.1. OPVs

OPV cells, especially BHJ and DSSC, are noted as the most popular applications of conjugated polymers employing stable SFTs units.^[31,74,95] In general, to achieve high device efficiency, it is the copolymers of SFTs with other aromatic heterocycles whereas not

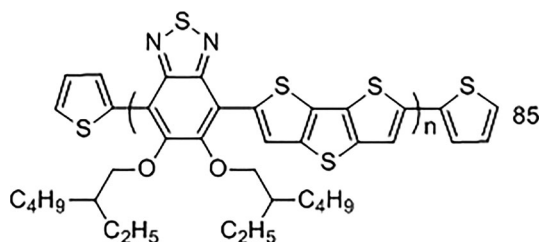


Figure 8. Molecular structures of polymer 85.

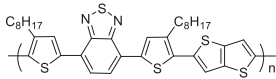
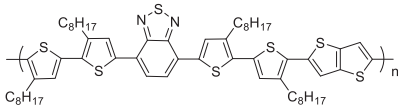
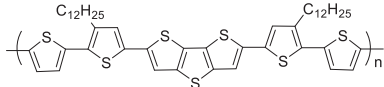
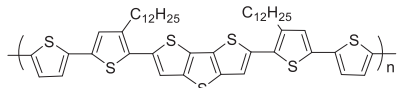
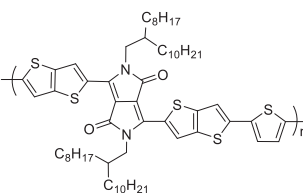
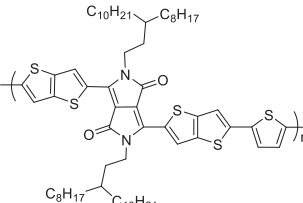
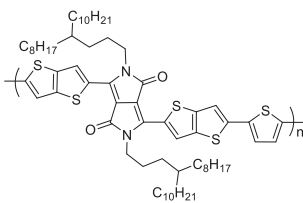
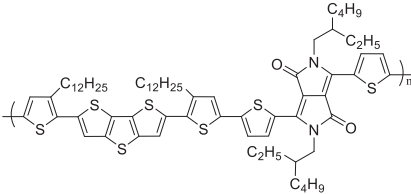
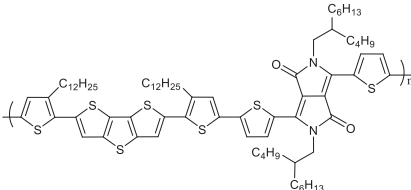
homopolymers, were chosen for obtaining broad and intense visible-light and even near-infrared range response through narrowing their E_g^{opt} and providing efficient photo-induced electron or hole transfer. The ubiquitous strategies are to construct enlarged conjugated structures and build D-A interaction.^[41,96] Although generally bringing little effect on the frontier orbital energy levels of polymers, attaching alkyl, alkoxy or other long chains (planar or blanching types) on the SFTs or corresponding heterocycles is quite necessary to get acceptable solubility.^[97–101] Surely, other factors for affecting polymer solubility are also required special attention, for example, the degree of polymerization, polarity of the attached substituents, skeleton rigidity, intermolecular interactions, etc.^[96]

Some typical SFTs-contained polymers for applying in OPVs are displayed in Figure 8 and Table 11. The modifications of alkyl chains on conjugated skeletons have gratifying effects on solubility, crystallinity, molecular orientation, and morphology of the co-polymers, which directly influence molecular orientation on the substrate, leading to improved PCE and materials processability. Noticeably, the face-on stacking intensively affects the OPVs efficiency owing to the improved carrier transfer based on the π - π stacking. Two-dimensional CI-XRD analysis has been conducted to investigate the crystallinity and specific molecular arrangement on the substrate in order to better understand the relationship between the alkyl chains' bulkiness and charge carrier mobility in the devices. It demonstrated that the relatively higher mobility for polymer 84 could be explained by the formation of small crystallites and their compactness on the film surface in comparison to polymers 82 and 83. The bulky alkyl chains can weaken the molecular aggregation by increasing the π - π stacking distance and decrease the crystallinity of the polymer.

Due to the difference in the charge property of atoms, the introduction of different atoms in repeating groups could produce different orbital energy levels, which can lead to the difference of V_{OC} values of OPVs devices. In addition, heterocycle bridges with different electron-donating ability can markedly tune the optical absorptions and orbital energy levels of polymers (as structures shown in Table 12).^[97,99,101–103] When thio-phenyl and selenophen units were inserted into polymer backbones, the PCEs will improve due to their smaller band gaps, better crystallinity, and carrier mobility.^[104–106] For polymers 96–98, their linear structures could generate conformational lock due to intra- and interchain noncovalent Coulombic interactions (S-O, S-N, hydrogen bond) resulting in strong molecular self-organization. And, the hole mobility was significantly improved by incorporating fluorine substituents into the polymer chain.^[107]

SFTs, acting as electron-donating units, play an important role of D and π -bridge in the polymer backbone to form the configuration of D-A, D- π -A, D-A-D-A for polymers

Table 11. Performances of OPVs devices based on polymers 75–88 according to tunable alkyl side chains.

Polymer	Structure	V_{oc}/V	$J_{sc}/(mA\ cm^{-2})$	FF	PCE/%
75		0.58	5.7	0.45	1.5
76		0.63	11.3	0.45	3.2
77		0.43	5.96	0.34	0.9
78		0.44	5.95	0.34	0.9
79		0.59	16.6	0.60	5.9
80		0.61	18.6	0.64	7.3
81		0.60	18.7	0.62	6.9
82		0.54	8.0	0.51	2.2
83		0.56	9.25	0.51	2.7

(continued)

Table 11. Continued.

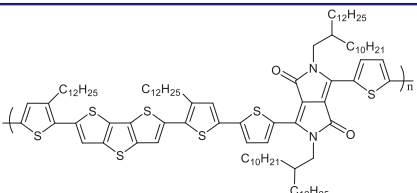
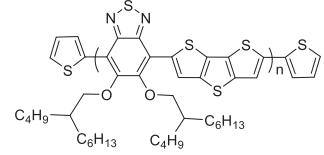
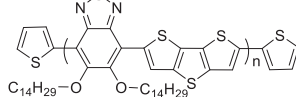
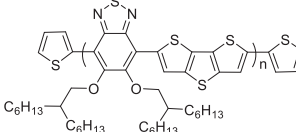
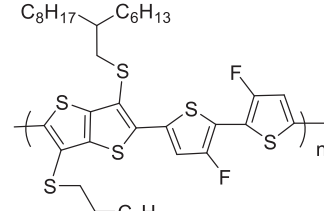
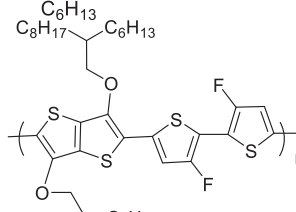
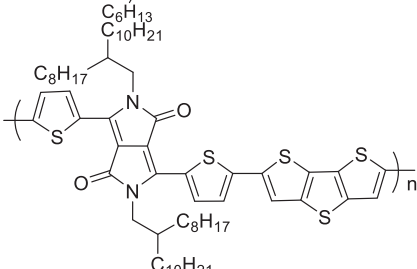
Polymer	Structure	V_{oc}/V	$J_{sc}/(\text{mA cm}^{-2})$	FF	PCE/%
84		0.59	7.1	0.63	2.7
86		0.91	12.14	0.48	5.4
87		0.65	10.05	0.53	3.4
88		0.92	11.68	0.53	5.7

Table 12. Performance of OPVs devices based on polymers 89–98 possessing different electron-donating units.

Polymer	Structure	V_{oc}/V	$J_{sc}/(\text{mA cm}^{-2})$	FF	PCE/%
89		0.76	8.54	0.73	4.73
90		0.44	8.31	0.57	2.15
91		0.63	11.40	0.71	5.10

(continued)

Table 12. Continued.

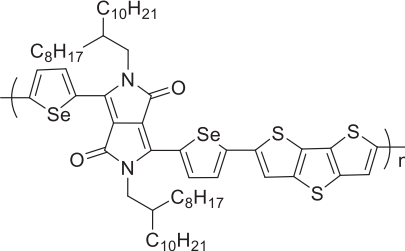
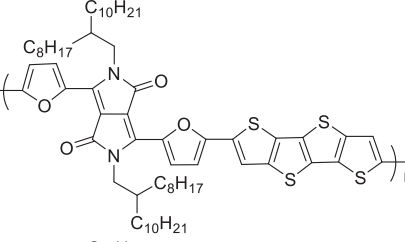
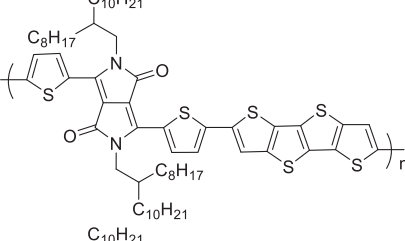
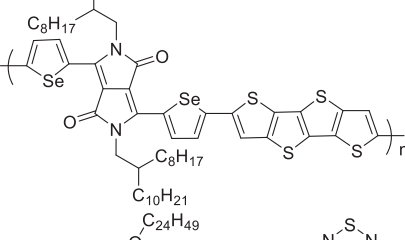
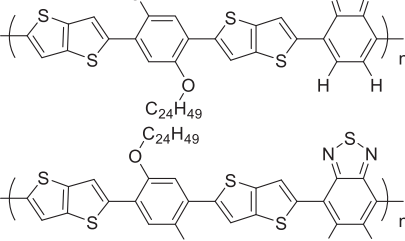
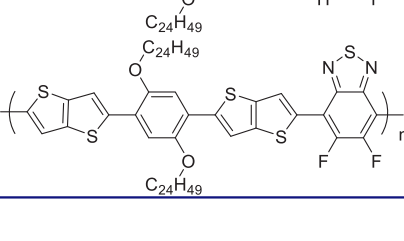

Polymer	Structure	V_{oc}/V	$J_{sc}/(\text{mA cm}^{-2})$	FF	PCE/%
92		0.53	11.60	0.66	4.05
93		0.63	10.55	0.58	3.84
94		0.60	11.76	0.64	4.55
95		0.58	15.62	0.62	5.68
96		0.61	9.82	0.60	3.54
97		0.71	11.70	0.63	5.20
98		0.74	13.30	0.63	6.40

Table 13. Performances of OPVs devices based on polymers 99–106 with configurations of D-A, D- π -A or D-A-D-A, where SFTs as donor and π -bridge units.

Polymer	Structure	V_{oc}/V	$J_{sc}/(\text{mA cm}^{-2})$	FF	PCE/%
99		0.86	15.30	0.70	9.21
100		0.78	10.56	0.62	5.05
101		0.57	8.90	0.59	3.00
102		0.58	15.00	0.61	5.40
103		0.65	1.47	0.31	0.29
104		0.60	5.15	0.45	1.39
105		0.67	3.76	0.39	0.97
106		0.77	4.18	0.37	1.19

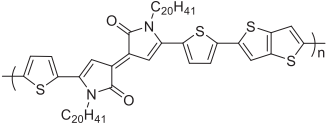
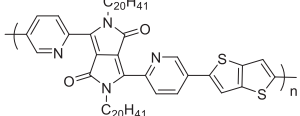
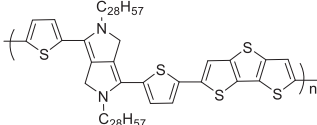
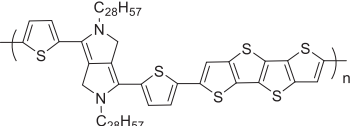
99–106 (structures are shown in Table 13).^[10,98,108,109] The band gaps of these polymers could effectively decrease to meet optimal 1.77 eV responding to both red and near-infrared ranges of solar light.^[110] The high planarity and rigidity of SFTs in conjugated polymers have been proven to be an effective approach to minimize the phase separation. The coplanar structure is beneficial to improve the π - π stacking and charge transfer property of the polymers in the solid state.^[111,112] As the OPVs performances of polymers 99–106 are summarized in Table 13. The extension of molecular coplanarity allows a much-delocalized HOMO distribution along the polymer backbone, which is to enhance intermolecular charge-carrier hopping. Electron transfer from D to A in polymers also can be effectively improved when small conjugated units were selected to link D and A units.

Nevertheless, designing an ideal polymer for OPVs is still a conundrum in the material science field. The characteristics of ideal polymers include better solution-processability, higher crystallinity, the smooth morphology, and strong π - π interaction via neighboring two polymers. Moreover, annealing temperatures, solution additives, different structural acceptors like PCBM for BHJ solar cell, and molecular arrangement on the substrate could also affect OPVs performance due to the state and morphology of the blend film. Fitted energy level of polymers is a key factor to meet the absorbance of the large range of the solar light spectrum. Fabrication and assembly technologies to outfit OPVs are still an active research orientation for different materials and under different environmental conditions.

4.2. OFETs and OTFTs

Different from small oligomer molecules containing SFTs units for OFETs application, their polymers have been extensively researched as active layers to fabricate OTFTs devices.^[86,113–117] However as the same, in order to achieve better device performance, D-A type molecular configuration of polymers employing SFTs units as electron-donating and π -bridge groups are still necessary. SFTs in polymer skeletons can adjust their HOMO energy levels, while A-type groups like DPP groups were then employed because they possess strong electron-withdrawing ability. As shown in Table 14, for DPP involved polymers 108–110, the conjugated degrees of repeating groups provide significant effects on the OTFTs performances.^[115–118] For polymer 107, it exhibits a specific ambipolar behavior unlike those of other polymers and displays two arrangements as shown in Figure 9. For different attachments that with similar molecular structures, like thienyl, selenophene and furan within polymers 111–114 in Table 15, researches indicated that polymer 114 based on furan possessed relative poor OTFTs performances due to the limited ability of providing electron of furan.

Table 14. Performances of OFETs devices of polymers 107–110 based on SFTs-contained structures.

Polymer	Structure	$\mu\text{h}/\text{cm}^{-2}\text{V}^{-1}\text{S}^{-1}$	$\mu\text{e}/\text{cm}^{-2}\text{V}^{-1}\text{S}^{-1}$	V_T/V	$I_{\text{on}}/I_{\text{off}}$ ratio
107		0.40	1.3×10^{-2}	14	10^3
108		0.35	–	–	–
109		1.18	–	–10	$>10^5$
110		1.19	–	0	10^6

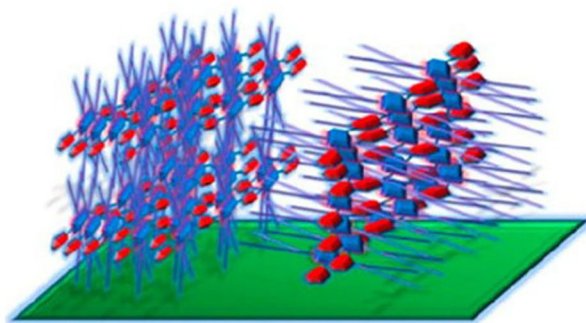


Figure 9. Schematic illustration of ambipolar molecular arrangements of polymer 107. Reprinted with permission from Zhang et al.^[115] Copyright 2014 American Chemistry Society.

Table 15. Performances of OFETs devices of polymers based on SFTs-contained and DPP units.

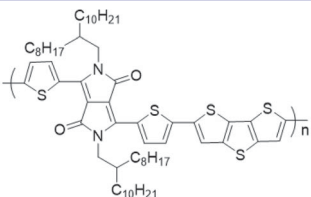
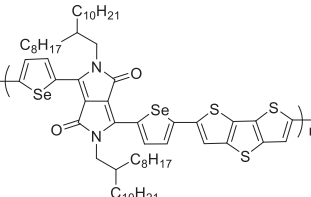
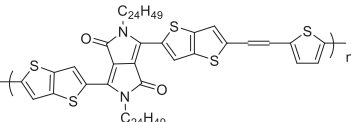
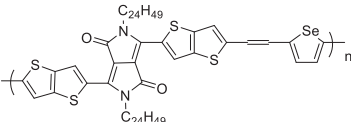
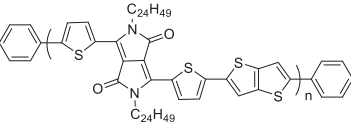
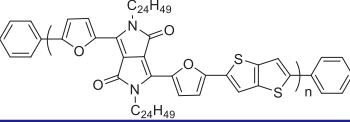
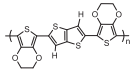
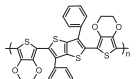
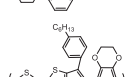
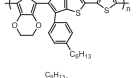
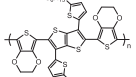
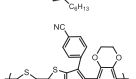
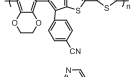
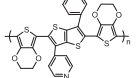
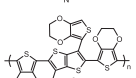
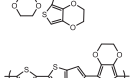
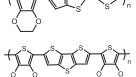
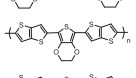
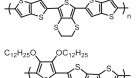
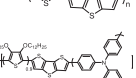
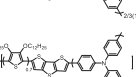
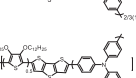
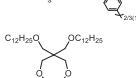
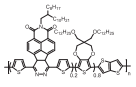
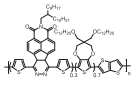
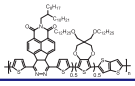
Polymer	Structure	$\mu\text{h}/\text{cm}^{-2}\text{V}^{-1}\text{S}^{-1}$	$\mu\text{e}/\text{cm}^{-2}\text{V}^{-1}\text{S}^{-1}$	V_{T}/V	$I_{\text{on}}/I_{\text{off}}$ ratio
91		0.23	1.5×10^{-2}	–	10^4
92		0.13	1.0×10^{-2}	–	10^3
111		0.44	–	–14	10^6
112		6.7×10^{-2}	–	–25	10^6
113		9.0×10^{-2}	2.0×10^{-2}	–26	–
114		4.0×10^{-2}	7.0×10^{-2}	–13	–

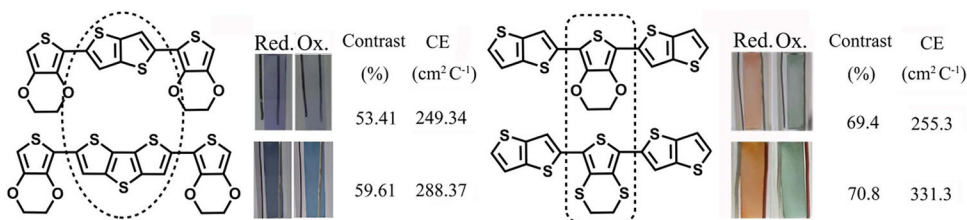
Table 17. Performances of EC devices based on SFTs-contained polymer films.

Polymer	Structure	Visible light		NIR light		Response time/s	
		$\Delta T/\%$	$CE/(\text{cm}^2 \text{C}^{-1})$	$\Delta T/\%$	$CE/(\text{cm}^2 \text{C}^{-1})$	Bleaching	Coloring
115		29.5	81.7	69.4	255.3	2.63	1.87
116		19.2	–	48.4	–	0.57	
117		–	–	60	–	2.7	2.0
118		–	–	60	–	0.96	1.63
119		23	120	62	440	0.90	0.34
120		16	190	50	324	1.10	0.35
121		38	93	64	234.6	0.36	
122		13.4	–	12	–	0.83	
123		34.4	153.0	59.6	288.4	0.97	1.31
124		29.5	81.7	69.4	255.3	2.63	1.87
125		29.9	133.2	70.8	331.3	0.72	1.98
129		44.7	370	79.4	406	–	
130		29.3	353	69.9	446	–	
131		14.2	68	42.8	140	–	
132		19.1	199	59.2	320	–	
133		43	361	78.6	353	–	
134		32.1	212	59.5	300	–	

(continued)

Table 17. Continued.

Polymer	Structure	Visible light		NIR light		Response time/s	
		$\Delta T/\%$	$CE/(\text{cm}^2 \text{C}^{-1})$	$\Delta T/\%$	$CE/(\text{cm}^2 \text{C}^{-1})$	Bleaching	Coloring
135		16.4	328	80.5	368	–	–
136		15.5	239	66.1	394	–	–
137		2.0	156	54.0	46.4	–	–

**Figure 11.** Molecular structures of ternary oligomers containing EDOT and TT or DTT units and the EC images and properties of their polymer film-coated ITO electrodes.

have highly limited by their planar and rigid conjugated structures. Thus, for this application, SFTs were mostly in combination with other hybrid units in copolymers, as shown in Figure 10 and Table 17.^[4,29,119–129]

Generally, most endeavors in this aspect to achieve better EC performance has been focused on incorporating SFTs units into main chains of PEDOTs through electrochemical polymerization of the oligomer precursors with SFTs and EDOT units as core unit or end-caps, respectively.^[121–124]

In the past five years, our, Meng's and other groups have reported a series of such polymers and investigated their structure–performance relationships as shown in Table 17.^[29,92,121,123,124,126,130,131] As listed in Figure 11, these show better EC performances than P(TT) ($36.8 \text{ cm}^2 \text{C}^{-1}$) due to the extension of the conjugated structure rearranged electron density and redox activity. When other functional groups (e.g., TPA, arylphenyl) were introduced into the β -position of TT units, much improved EC performances were achieved owing to the lower bandgap and broader absorption.

In addition, some complex polymers 129–135 that employ other D-type or A-type groups with flexible alkyl or alkoxy chains were also demonstrated as good EC materials.^[5,125,127–130] For instance, A-type units are inserted in P(TT), causing a lower LUMO energy level and higher residual absorption, leading to higher ECs performance.

ECs of based on SFTs-contained copolymers can be noted as a much promising field beyond their use in OPVs, especially considering current preference for flexible displays and smart life, where the inorganic materials have severe limitations. There are many similar design philosophies about material structure and device fabrication between such fields. Moreover, in light of the great success of aqueous dispersions of PEDOT/PSS and their flexible ECs films, chemically oxidative homopolymerization of above-mentioned

Table 18. Performances of OLEDs devices based on copolymers 138–140.

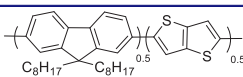
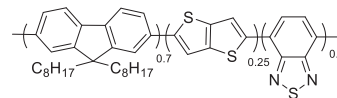
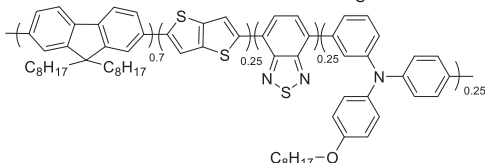
Polymer	Structure	Luminance ^{max} /cd m ⁻²	EL efficiency ^{max} /cd A ⁻¹
138		970	0.32
139		1450	1.35
140		3000	0.64

Table 19. TE performances of polymer films containing TT structure.

Polymer	Temperature/°C	σ /(S cm ⁻¹)	S /(μ V K ⁻¹)
P(TT)	25	0.42	75
	-75	0.04	51
P(TT/2Cz-D) = 10:1	-75	0.12	169
P(TT/2Cz-D) = 3:1	-75	0.26	85

oligomers or copolymerization of SFTs with EDOTs will be a promising research direction. Further interesting results also may be found if they are introduced into hydrogel bioelectronics and applied through emerging film-forming technologies.^[132]

4.4. OLEDs

OLEDs, employing π -conjugated polymers as active layers as shown in Figure 4, have been rapidly developed in the past decades due to their highly active photoluminescence (PL) or electroluminescence (EL), along with flexibility and low energy consumption.^[133] As a typical electron-rich unit or π -bridge, TT has been introduced in electroluminescent copolymers (Table 18) with alkyl fluorenyl groups through Suzuki polymerization, which is beneficial to improve the hole affinity of copolymers.^[133] With the help of further incorporation of electron-deficient benzothiadiazole and electron-rich triphenylamine moieties in the main chains (Table 18), the film EL efficiency meets greater improvement due to optimizing electron- and hole-transporting, better solubility and thermal stability.^[134]

Although their applications in this field are still quite a few, enlightened by abundant design concepts of molecular structures and device constructions in OPVs and OFETs, SFTs and their polymers may find further development in OLEDs.

4.5. TEs

TEs devices have functionality for green power generation from waste heat and solid-state refrigeration. The application of organic semiconductor polymers in this field is a challenging but extraordinarily interesting branch which has gained wide attention in the past decade since our concentrative research on PEDOT in 2008.^[135–138] The key factor for evaluating TE performances of materials is the so-called dimensionless thermoelectric figure-of-merit (ZT) as defined by Eq. 3:

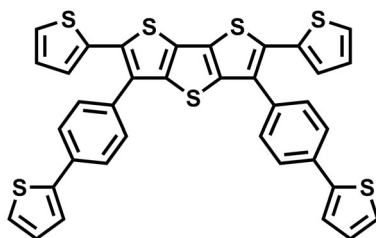


Figure 12. Molecular structure of Th₄DTT for applying in capacitor.

$$ZT = \frac{(\sigma S^2)T}{K} \quad (3)$$

where S is the Seebeck coefficient, σ is the electrical conductivity, T is the absolute temperature, and K is the thermal conductivity. Also, power factor P ($=\sigma S^2$) is sometimes used. A commercial TE material should reach a ZT value of 1.0 at operating temperatures. Although it is still an unreachable level for organic TEs, we and others have improved the data from 10^{-4} to 10^{-1} orders of magnitude.^[139] As a typical example, the ZT value of PEDOTs-based TE films has reached ca. 0.5, making polythiophenes derivatives attracted most of the interest in this field.^[139,140] In 2011, our group investigated the TE performance of electrosynthesized free-standing P(TT) film and fabricated simple devices (Figure 4).^[140] Through combining with 1,12-bis(carbazolyl)-dodecane (2Cz-D) into free-standing copolymer films, a dependence between electrical conductivities and molar ratios of TT and 2Cz-D monomers can be found.^[141,142] When the ratio was decreased from TT/2Cz-D of 10:1 to 3:1, higher S and p values than P(TT) films were achieved (Table 19). But owing to their low conductivity and molecular complexity than PEDOTs, for a long time, there is no further development about SFTs-contained TE polymers. We believe there may be two ways to promote this field, embeddings SFTs units into PEDOTs or other preferred organic TE skeletons, and fabricating regular assembly structures with bulk-phase micro-/nano-scale nanofiber morphology from small molecules, oligomers or polymers.

4.6. Supercapacitors

Capacitor application is extremely important for energy storage and to meet current green power tendency. Supercapacitors based on the electrochemical mechanism with the help of thin-film conjugated polymer electrodes (Figure 4) have achieved wide interest from our and other groups in recent years.^[143–146] Ates et al.^[146] found a specific capacitance value of 0.18 mFcm^{-2} for a double eletctro-active layer capacitor based on P(Th₄DTT) (Figure 12) and a much higher data about 4.43 mFcm^{-2} for that based on P(Th₄DTT)/multi-walled carbon nanotube (MWCNT) composites. These composites also showed long-term stability, remaining 87.37% efficiency of SFTs-contained conjugated polymers. The inherent structural and electronic advantages and high energy density of MWCNTs played a significant role in such results. Also, the interchain interactions and mesoporous structures are vital to achieve high supercapacitor performances. Nevertheless, the properties of individual conjugation structure, charge-discharge ability, intermolecular interactions, and extent of disorder for materials, the development of polymers-based capacitors still face severe difficulties.^[147–149] The design of

electrochemically synthesized polymer films from oligomers containing both SFTs and preferred groups (e.g., EDOT) as well as their composites with preferred carbon materials could be seen as a potential research direction.

5. Conclusions and outlook

In summary, we systematically discussed the structure–performance relationships of SFTs-contained oligomers and polymers are related to wide applications, especially OPVs, OFETs, OLEDs, and ECs. When integrated with other constitutional units such as penta-heterocycles, phenyl derivatives, and polycyclic aromatic units, etc., SFTs units as the π -conjugated cores or bridges in the molecular skeletons will bring enhanced charge carrier generation and transfer efficiency and thereby improved device performances.

In general, regardless of special device applications, three critical molecular design strategies have been adopted. On one hand, enlargement of the conjugated molecular skeleton via tuning thiophenyl numbers of SFTs or attaching other conjugated structural units at horizontal and/or side directions has been utilized to achieve much planar structures and better intramolecular charge mobility. On another hand, D-A constructions and functional side chain modification are developed to meet much wide or special objectives. Last, alteration of alkyl substituents on the conjugated skeleton units can not only improve molecular solubility but also modulate the molecular chain orientation, intermolecular interaction, and solid-state morphology. In view of different applications, other cases also should be given special considerations to get high performances. For example, a broad molecular absorption in the visible-light regions is quite important for OPVs, an effective D-A or n-p structure is necessary for OFETs, a good conductivity is favorable to both ECs and TEs, and variable color transition is required for ECs.

Besides these ways, some new design principles can be introduced to this field. For example, since SFTs have flat structural stereo-structures, their oligomers or polymers could be constructed into well-defined stacking micro-/nano-scale structures with diverse dimensional conformations via strong intermolecular interactions. Also, the presence of abundant electrons offers many possibilities to design complex composites with other functional compounds via hydrogen bonds, chalcogen interaction, and others. Inspired by supramolecular or coordinative chemistry, nanotechnology, etc., besides remarkable applications mentioned above, these novel materials and bulk phase structures may find opportunities in optoelectronic sensors, flexible electronics, and even biology detection or pharmacy therapy of diseases.

Moreover, another important factor for realizing much high-performance devices is selective fabrication or posttreatment technology. Recently, adding external molecular doping solvent is demonstrated as an effective way to improve the stability and optimize carrier transport properties of SFTs-contained oligomers and polymers.^[150] It is believed that if SFTs-contained oligomers or polymers can be compatible with forefront technologies (e.g., 3D printing), as well as assembly or hybrid combination with different type semiconductors (e.g., forming heterogeneous junction) meet much promising performances and commercial applications.

Nevertheless, there are still many challenges for SFTs-based materials to realize above-mentioned prospect considering more and more complex molecular synthesis or

precise polymerization control, and optimal matching with other components in devices with efficiency bottleneck. These problems exist in almost the whole field of organic electronics which need cooperation between material scientists, technique engineers and theoretical researchers to overcome.

Funding

This work was supported by the National Natural Science Foundation of China under Grant 51603095 and 51863009; the scholarship from China Scholarship Council under Grant 201808360327; Natural Science Foundation of Jiangxi Province under Grant 20192BAB216012; Scientific Fund of Jiangxi Science & Technology Normal University under Grant 2016QNBjRC003; Jiangxi Educational Committee for a Postgraduate Innovation Program Grant under Grant YC2018-X29.

References

- [1] Ewa, S.-B.; Marzena, G.-Z.; Michal, K.; Henryk, J.; Mariola, S.; Danuta, S. New Naphthalene Diimide-Based Compounds Containing Triarylamine Units and Imine Linkages: Thermal, Optical and Electrochemical Properties. *Synth. Met.* **2011**, *161*, 2268–2279. DOI: [10.1016/j.synthmet.2011.08.032](https://doi.org/10.1016/j.synthmet.2011.08.032).
- [2] Wu, W.-P.; Liu, Y.-Q.; Zhu, D.-B. π -Conjugated Molecules with Fused Rings for Organic Field-Effect Transistors: Design, Synthesis and Applications. *Chem. Soc. Rev.* **2010**, *39*, 1489–1502. DOI: [10.1039/B813123F](https://doi.org/10.1039/B813123F).
- [3] Cinar, M. E.; Ozturk, T. Thienothiophenes, Dithienothiophenes, and Thienoacenes: Syntheses, Oligomers, Polymers, and Properties. *Chem. Rev.* **2015**, *115*, 3036–3140. DOI: [10.1021/cr500271a](https://doi.org/10.1021/cr500271a).
- [4] Gunbas, G.; Toppare, L. Electrochromic Conjugated Polyheterocycles and Derivatives—Highlights from the Last Decade towards Realization of Long Lived Aspirations. *Chem. Commun.* **2012**, *48*, 1083–1101. DOI: [10.1039/C1CC14992J](https://doi.org/10.1039/C1CC14992J).
- [5] Cho, C.-M.; Neo, W.-T.; Ye, Q.; Lu, X.-H.; Xu, J.-W. Dithienothiophene-Based Triphenylamine-Containing Branched Copolymers for Electrochromic Applications. *ChemPlusChem* **2015**, *80*, 1306–1311. DOI: [10.1002/cplu.201500192](https://doi.org/10.1002/cplu.201500192).
- [6] Turkoglu, G.; Cinar, M. E.; Ozturk, T. Thiophene-Based Organic Semiconductors. *Top. Curr. Chem.* **2017**, *375*, 84–128. DOI: [10.1007/s41061-017-0174-z](https://doi.org/10.1007/s41061-017-0174-z).
- [7] Chen, S.-L.; Qiao, X.-L.; Li, H.-P.; Li, H.-X. Acceptor-Donor-Acceptor Type Small Molecular Low Band Gap Organic Semiconductors Containing 2-Dicyanomethylen-3-Cyano-4,5,5-Trimethyl-Dihydrofuran. *Chin. J. Chem.* **2015**, *33*, 934–938. DOI: [10.1002/cjoc.201400811](https://doi.org/10.1002/cjoc.201400811).
- [8] Xiao, K.; Liu, Y.-Q.; Qi, T.; Zhang, W.; Wang, F.; Gao, J.-H.; Qiu, W.-F.; Ma, Y.-Q.; Cui, G.-L.; Chen, S.-Y.; et al. A Highly π -Stacked Organic Semiconductor for Field-Effect Transistors Based on Linearly Condensed Pentathienoacene. *J. Am. Chem. Soc.* **2005**, *127*, 13281–13286. DOI: [10.1021/ja052816b](https://doi.org/10.1021/ja052816b).
- [9] Wang, C.-Z.; Do, J.-H.; Akther, T.; Feng, X.; Matsumoto, T.; Tanaka, J.; Redshaw, C.; Yamato, T. Synthesis and Fluorescence Emission Properties of D- π -D Monomers Based on Dithieno[3,2-*b*:2',3'-*d*]Thiophene. *J. Lumin.* **2017**, *188*, 388–393. DOI: [10.1016/j.jlumin.2017.04.060](https://doi.org/10.1016/j.jlumin.2017.04.060).
- [10] Patil, A. V.; Lee, W.-H.; Kim, K.; Park, H.; Kang, I. N.; Lee, S.-H. Synthesis and Photovoltaic Properties of Narrow Band Gap Copolymers of Dithieno[3,2-*b*:2',3'-*d*] Thiophene and Diketopyrrolopyrrole. *Polym. Chem.* **2011**, *2*, 2907–2916. DOI: [10.1039/c1py00274k](https://doi.org/10.1039/c1py00274k).
- [11] Lin, C.-J.; Lee, W.-Y.; Lu, C.; Lin, H.-W.; Chen, W.-C. Biaxially Extended Thiophene-Fused Thiophene Conjugated Copolymers for High Performance Field Effect Transistors. *Macromolecules* **2011**, *44*, 9565–9573. DOI: [10.1021/ma202017q](https://doi.org/10.1021/ma202017q).

- [12] Vyprachticky, D.; Demirtas, L.; Dzhabarov, V.; Pokorna, V.; Ertas, E.; Ozturk, T.; Cimrova, V. New Copolymers with Thieno[3,2-*b*]Thiophene or Dithieno[3,2-*b*:2',3'-*d*]Thiophene Units Possessing Electron-Withdrawing 4-Cyanophenyl Groups: Synthesis and Photophysical, Electrochemical, and Electroluminescent Properties. *J. Polym. Sci. Part A: Polym. Chem.* **2017**, *55*, 2629–2638. DOI: [10.1002/pola.28657](https://doi.org/10.1002/pola.28657).
- [13] Hou, J.-H.; Inganäs, O.; Friend, R. H.; Gao, F. Organic Solar Cells Based on Non-Fullerene Acceptors. *Nat. Mater.* **2018**, *17*, 119–128. DOI: [10.1038/nmat5063](https://doi.org/10.1038/nmat5063).
- [14] Jung, J.-W.; Liu, F.; Russell, T. P.; Jo, W. H. A High Mobility Conjugated Polymer Based on Dithienothiophene and Diketopyrrolopyrrole for Organic Photovoltaics. *Energy Environ. Sci.* **2012**, *5*, 6857–6861. DOI: [10.1039/c2ee21149a](https://doi.org/10.1039/c2ee21149a).
- [15] Sannasi, V.; Jeyakumar, D. Effect of Co-Monomers on Triphenylamine-Thiazolothiazole-Based Donor-Acceptor Copolymers: Synthesis and Their Optical Properties. *ChemistrySelect* **2017**, *2*, 1992–1998. DOI: [10.1002/slct.201601496](https://doi.org/10.1002/slct.201601496).
- [16] Priyanka, P.; Vegiraju, S.; Lin, J.-Y.; Ni, J.-S.; Huang, H.-Y.; Agustin, R. D.; Yau, S. L.; Lin, T.-C.; Chen, M.-C. Synthesis and Characterization of Two-Photon Active Chromophores Based on Asymmetrically Substituted Tetrathienoacene Scaffolds. *Dyes Pigments* **2016**, *133*, 65–72. DOI: [10.1016/j.dyepig.2016.05.038](https://doi.org/10.1016/j.dyepig.2016.05.038).
- [17] Chen, S.; Jacobs, D. L.; Xu, J.-K.; Li, Y.-X.; Wang, C.-Y.; Zang, L. 1D Nanofiber Composites of Perylene Diimides for Visible-Light-Driven Hydrogen Evolution from Water. *RSC Adv.* **2014**, *4*, 48486–48491. DOI: [10.1039/C4RA09258A](https://doi.org/10.1039/C4RA09258A).
- [18] Chen, S.; Wang, C.; Bunes, B. R.; Li, Y.-X.; Wang, C.-Y.; Zang, L. Enhancement of Visible-Light-Driven Photocatalytic H₂ Evolution from Water over g-C₃N₄ through Combination with Perylene Diimide Aggregates. *Appl. Catal. A Gen.* **2015**, *498*, 63–68. DOI: [10.1016/j.apcata.2015.03.026](https://doi.org/10.1016/j.apcata.2015.03.026).
- [19] Zang, L.; Che, Y.; Moore, J. S. One-Dimensional Self-Assembly of Planar π -Conjugated Molecules: Adaptable Building Blocks for Organic Nanodevices. *Acc. Chem. Res.* **2008**, *41*, 1596–1608. DOI: [10.1021/ar800030w](https://doi.org/10.1021/ar800030w).
- [20] Che, Y.; Yang, X.-M.; Balakrishnan, K.; Zuo, J.-M.; Zang, L. Highly Polarized and Self-Waveguided Emission from Single-Crystalline Organic Nanobelts. *Chem. Mater.* **2009**, *21*, 2930–2934. DOI: [10.1021/cm9007409](https://doi.org/10.1021/cm9007409).
- [21] Chen, S.; Slattum, P.; Wang, C.-Y.; Zang, L. Self-Assembly of Perylene Imide Molecules into 1D Nanostructures: Methods, Morphologies, and Applications. *Chem. Rev.* **2015**, *115*, 11967–11998. DOI: [10.1021/acs.chemrev.5b00312](https://doi.org/10.1021/acs.chemrev.5b00312).
- [22] Datar, A.; Oitker, R.; Zang, L. Surface-Assisted One-Dimensional Self-Assembly of a Perylene Based Semiconductor Molecule. *Chem. Commun.* **2006**, *15*, 1649–1651. DOI: [10.1039/b518060k](https://doi.org/10.1039/b518060k).
- [23] Che, Y.; Yang, X.-M.; Liu, G.-L.; Yu, C.; Ji, H.-W.; Zuo, J.-M.; Zhao, J.-C.; Zang, L. Ultrathin *n*-Type Organic Nanoribbons with High Photoconductivity and Application in Optoelectronic Vapor Sensing of Explosives. *J. Am. Chem. Soc.* **2010**, *132*, 5743–5750. DOI: [10.1021/ja909797q](https://doi.org/10.1021/ja909797q).
- [24] Wang, X.-D.; Meng, F.-L.; Wang, T.-Z.; Li, C.-C.; Tang, H.-T.; Gao, Z.-M.; Li, S.; Jiang, F.-X.; Xu, J.-K. High Performance of PEDOT:PSS/SiC-NWs Hybrid Thermoelectric Thin Film for Energy Harvesting. *J. Alloy. Compd.* **2018**, *734*, 121–129. DOI: [10.1016/j.jallcom.2017.11.013](https://doi.org/10.1016/j.jallcom.2017.11.013).
- [25] Gu, H.; Ming, S.-L.; Lin, K.-W.; Chen, S.; Liu, X.-M.; Lu, B.-Y.; Xu, J.-K. Isoindigo as an Electron-Deficient Unit for High-Performance Polymeric Electrochromics. *Electrochim. Acta* **2018**, *260*, 772–782. DOI: [10.1016/j.electacta.2017.12.033](https://doi.org/10.1016/j.electacta.2017.12.033).
- [26] Liu, J.; Jia, Y.-H.; Jiang, Q.-L.; Jiang, F.-X.; Li, C.-C.; Wang, X.-D.; Liu, P.; Liu, P.-P.; Hu, F.; Du, Y.-K.; et al. Highly Conductive Hydrogel Polymer Fibers toward Promising Wearable Thermoelectric Energy Harvesting. *ACS Appl. Mater. Interfaces* **2018**, *10*, 44033–44040. DOI: [10.1021/acsami.8b15332](https://doi.org/10.1021/acsami.8b15332).
- [27] Aragón, J.; Viruela, P. M.; Orti, E. From Linear Quaterthiophene to Sulflower: A Comparative Theoretical Study. *J. Mol. Struct. Theochem.* **2009**, *912*, 27–31. DOI: [10.1016/j.theochem.2009.03.021](https://doi.org/10.1016/j.theochem.2009.03.021).

- [28] Liu, Y.; Sun, X.-N.; Di, C.-A.; Liu, Y.-Q.; Du, C.-Y.; Lu, K.; Ye, S.-H.; Yu, G. Hexathienoacene: Synthesis, Characterization, and Thin-Film Transistors. *Chem. Asian J.* **2010**, *5*, 1550–1554. DOI: [10.1002/asia.201000001](https://doi.org/10.1002/asia.201000001).
- [29] Xue, Y.; Xue, Z.-X.; Zhang, W.-W.; Zhang, W.-N.; Chen, S.; Lin, K.-W.; Xu, J.-K. Enhanced Electrochromic Performances of Polythieno[3,2-*b*]Thiophene with Multicolor Conversion via Embedding EDOT Segment. *Polymer* **2018**, *159*, 150–156. DOI: [10.1016/j.polymer.2018.11.018](https://doi.org/10.1016/j.polymer.2018.11.018).
- [30] Zhang, Y.-X.; Cai, X.; Bian, Y.-Z.; Li, X.-Y.; Jiang, J.-Z. Heteroatom Substitution of Oligothienoacenes: From Good p-Type Semiconductors to Good Ambipolar Semiconductors for Organic Field-Effect Transistors. *J. Phys. Chem. C* **2008**, *112*, 5148–5159. DOI: [10.1021/jp710123r](https://doi.org/10.1021/jp710123r).
- [31] Kwon, T.-H.; Armel, V.; Nattestad, A.; MacFarlane, D. R.; Bach, U.; Lind, S. J.; Gordon, K.; C.; Tang, W.-H.; Jones, D. J.; Holmes, A. B. Dithienothiophene (DTT)-Based Dyes for Dye-Sensitized Solar Cells: Synthesis of 2,6-Dibromo-DTT. *J. Org. Chem.* **2011**, *76*, 4088–4093. DOI: [10.1021/jo2001484](https://doi.org/10.1021/jo2001484).
- [32] Kim, J. S.; Kim, B.-Y.; Kim, U.-Y.; Shin, H.; Nam, J. S.; Roh, D. H.; Park, J.-H.; Kwon, T.-H. Molecular Engineering for Enhanced Charge Transfer in Thin-Film Photoanode. *ACS Appl. Mater. Interfaces* **2017**, *9*, 34812–34820. DOI: [10.1021/acsami.7b08098](https://doi.org/10.1021/acsami.7b08098).
- [33] Yoon, G. B.; Kwon, H.-Y.; Jung, S.-K.; Lee, J.-K.; Lee, J. Effect of Donor Building Blocks on the Charge-Transfer Characteristics of Diketopyrrolopyrrole-Based Donor-Acceptor-Type Semiconducting Copolymers. *ACS Appl. Mater. Interfaces* **2017**, *9*, 39502–39510. DOI: [10.1021/acsami.7b11897](https://doi.org/10.1021/acsami.7b11897).
- [34] Jeong, M.; Chen, S.-S.; Lee, S. M.; Wang, Z.-W.; Yang, Y.-K.; Zhang, Z.-G.; Zhang, C.-F.; Xiao, M.; Li, Y.-F.; Yang, C. Feasible D1-A-D2-A Random Copolymers for Simultaneous High-Performance Fullerene and Nonfullerene Solar Cells. *Adv. Energy Mater.* **2018**, *8*, 1702166. DOI: [10.1002/aenm.201702166](https://doi.org/10.1002/aenm.201702166).
- [35] Shin, E.-Y.; Cho, H. J.; Jung, S.; Yang, C.; Noh, Y.-Y. A High-*k* Fluorinated P(VDF-TrFE)-*g*-PMMA Gate Dielectric for High-Performance Flexible Field-Effect Transistors. *Adv. Funct. Mater.* **2018**, *28*, 1704780. DOI: [10.1002/adfm.201704780](https://doi.org/10.1002/adfm.201704780).
- [36] Ho, D.; Jeon, M.; Kim, H.; Gidron, O.; Kim, C.; Seo, S. Y. Solution-Processable Dithieno[3,2-*b*:2',3'-*d*]Thiophene Derivatives for Organic Thin-Film Transistors and Complementary-Like Inverters. *Org. Electron* **2018**, *52*, 356–363. DOI: [10.1016/j.orgel.2017.11.023](https://doi.org/10.1016/j.orgel.2017.11.023).
- [37] Kini, G. P.; Oh, S.; Abbas, Z.; Rasool, S.; Jahandar, M.; Song, C. E.; Lee, S. K.; Shin, W. S.; So, W.-W.; Lee, J.-C. Effects on Photovoltaic Performance of Dialkyloxy-Benzothiadiazole Copolymers by Varying the Thienoacene Donor. *ACS Appl. Mater. Interfaces* **2017**, *9*, 12617–12628. DOI: [10.1021/acsami.6b12670](https://doi.org/10.1021/acsami.6b12670).
- [38] Li, Z.; Malenfant, P.; Tao, Y.; Ding, J.-F. Thermochromic and Photovoltaic Properties of an Alternating Copolymer of Dithieno[3,2-*b*:2',3'-*d*]Thiophene and Thieno[3,4-*c*]Pyrrole-4,6-Dione. *Macromol. Chem. Phys.* **2013**, *214*, 447–452. DOI: [10.1002/macp.201200468](https://doi.org/10.1002/macp.201200468).
- [39] Hasegawa, T.; Takeya, J. Organic Field-Effect Transistors Using Single Crystals. *Sci. Technol. Adv. Mater.* **2009**, *10*, 024314. DOI: [10.1088/1468-6996/10/2/024314](https://doi.org/10.1088/1468-6996/10/2/024314).
- [40] Günes, S.; Neugebauer, H.; Sariciftci, N. S. Conjugated Polymer-Based Organic Solar Cells. *Chem. Rev.* **2007**, *107*, 1324–1338. DOI: [10.1021/cr050149z](https://doi.org/10.1021/cr050149z).
- [41] Clarke, T. M.; Durrant, J. R. Charge Photogeneration in Organic Solar Cells. *Chem. Rev.* **2010**, *110*, 6736–6767. DOI: [10.1021/cr900271s](https://doi.org/10.1021/cr900271s).
- [42] Dong, X.; Tian, H.-K.; Xie, Z.-Y.; Geng, Y.-H.; Wang, F.-S. Donor-Acceptor Conjugated Polymers Based on Two-Dimensional Thiophene Derivatives for Bulk Heterojunction Solar Cells. *Polym. Chem.* **2017**, *8*, 421–430. DOI: [10.1039/C6PY01767C](https://doi.org/10.1039/C6PY01767C).
- [43] Mamillapalli, N. C.; Vegiraju, S.; Priyanka, P.; Lin, C.-Y.; Luo, X.-L.; Tsai, H.-C.; Hong, S.-H.; Ni, J.-S.; Lien, W.-C.; Kwon, G.; et al. Solution-Processable End-Functionalized Tetrathienoacene Semiconductors: Synthesis, Characterization and Organic Field Effect Transistors Applications. *Dyes Pigments* **2017**, *145*, 584–590. DOI: [10.1016/j.dyepig.2017.06.017](https://doi.org/10.1016/j.dyepig.2017.06.017).
- [44] Vegiraju, S.; Huang, D.-Y.; Priyanka, P.; Li, Y.-S.; Luo, X.-L.; Hong, S.-H.; Ni, J.-S.; Tung, S.-H.; Wang, C.-L.; Lien, W.-C.; et al. High Performance Solution-Processable

- Tetrathienoacene (TTAR) Based Small Molecules for Organic Field Effect Transistors (OFETs). *Chem. Commun.* **2017**, 53, 5898–5901. DOI: [10.1039/C7CC02714A](https://doi.org/10.1039/C7CC02714A).
- [45] Tang, W.-H.; Singh, S. P.; Ong, K. H.; Chen, Z.-K. Synthesis of Thieno[3,2-*b*]Thiophene Derived Conjugated Oligomers for Field-Effect Transistors Applications. *J. Mater. Chem.* **2010**, *20*, 1497–1505. DOI: [10.1039/b920112b](https://doi.org/10.1039/b920112b).
- [46] Sun, Y.-M.; Ma, Y.-Q.; Liu, Y.-Q.; Lin, Y.-Y.; Wang, Z.-Y.; Wang, Y.; Di, C.-A.; Xiao, K.; Chen, X.-M.; Qiu, W.-F.; et al. High-Performance and Stable Organic Thin-Film Transistors Based on Fused Thiophenes. *Adv. Funct. Mater.* **2006**, *16*, 426–432. DOI: [10.1002/adfm.200500547](https://doi.org/10.1002/adfm.200500547).
- [47] Li, X.-C.; Sirringhaus, H.; Garnier, F.; Holmes, A. B.; Moratti, S. C.; Feeder, N.; Clegg, W.; Teat, S. J.; Friend, R. H. A Highly π -Stacked Organic Semiconductor for Thin Film Transistors Based on Fused Thiophenes. *J. Am. Chem. Soc.* **1998**, *120*, 2206–2207. DOI: [10.1021/ja9735968](https://doi.org/10.1021/ja9735968).
- [48] Vegiraju, S.; He, G.-Y.; Kim, C.; Priyanka, P.; Chiu, Y.-J.; Liu, C.-W.; Huang, C.-Y.; Ni, J.-S.; Wu, Y.-W.; Chen, Z.-H.; et al. Solution-Processable Dithienothiophenoquinoid (DTTQ) Structures for Ambient-Stable n-Channel Organic Field Effect Transistors. *Adv. Funct. Mater.* **2017**, *27*, 1606761. DOI: [10.1002/adfm.201606761](https://doi.org/10.1002/adfm.201606761).
- [49] Wu, Q.-H.; Qiao, X.-L.; Huang, Q.-L.; Li, J.; Xiong, Y.; Gao, X.-K.; Li, H.-X. High-Performance n-Channel Field Effect Transistors Based on Solution-Processed Dicyanomethylene-Substituted Tetrathienoquinoid. *RSC Adv.* **2014**, *4*, 16939–16943. DOI: [10.1039/C3RA47095D](https://doi.org/10.1039/C3RA47095D).
- [50] Wang, Y.; Liu, D.-D.; Ikeda, S.; Kumashiro, R.; Nouch, R.; Xu, Y.-X.; Shang, H.; Ma, Y.-G.; Tanigaki, K. Ambipolar Behavior of 2,5-Diphenyl-1,4-Distyrylbenzene Based Field Effect Transistors: An Experimental and Theoretical Study. *Appl. Phys. Lett.* **2010**, *97*, 033305. DOI: [10.1063/1.3465659](https://doi.org/10.1063/1.3465659).
- [51] Ahmed, M. O.; Wang, C.-M.; Keg, P.; Pisula, W.; Lam, Y.-M.; Ong, B. S.; Ng, S.-C.; Chen, Z.-K.; Mhaisalkar, S. G. Thieno[3,2-*b*]Thiophene Oligomers and Their Applications as p-Type Organic Semiconductors. *J. Mater. Chem.* **2009**, *19*, 3449–3456. DOI: [10.1039/b900979e](https://doi.org/10.1039/b900979e).
- [52] Liu, Y.; Di, C.-A.; Du, C.-Y.; Liu, Y.-Q.; Lu, K.; Qiu, W.-F.; Yu, G. Synthesis, Structures, and Properties of Fused Thiophenes for Organic Field-Effect Transistors. *Chem. Eur. J.* **2010**, *16*, 2231–2239. DOI: [10.1002/chem.200902755](https://doi.org/10.1002/chem.200902755).
- [53] Wang, C.-Z.; Do, J.-H.; Akther, T.; Feng, X.; Horsburgh, L.; Elsegood, M. R. J.; Redshaw, C.; Yamato, T. D- π -D Chromophores Based on Dithieno[3,2-*b*:2',3'-*d*]Thiophene (DTT): Potential Application in the Fabrication of Solar Cell. *Tetrahedron* **2017**, *73*, 307–312. DOI: [10.1016/j.tet.2016.11.077](https://doi.org/10.1016/j.tet.2016.11.077).
- [54] Chen, M.-C.; Vegiraju, S.; Huang, C.-M.; Huang, P.-Y.; Prabakaran, K.; Yau, S. L.; Chen, W.-C.; Peng, W.-T.; Chao, I.; Kim, C.; et al. Asymmetric Fused Thiophenes for Field-Effect Transistors: Crystal Structure-Film Microstructure-Transistor Performance Correlations. *J. Mater. Chem. C* **2014**, *2*, 8892–8902. DOI: [10.1039/C4TC01454E](https://doi.org/10.1039/C4TC01454E).
- [55] Liu, Y.; Wang, Y.; Wu, W.-P.; Liu, Y.-Q.; Xi, H.-X.; Wang, L.-M.; Qiu, W.-F.; Lu, K.; Du, C.-Y.; Yu, G. Synthesis, Characterization, and Field-Effect Transistor Performance of Thieno[3,2-*b*]Thieno[2',3':4,5]Thieno[2,3-*d*]Thiophene Derivatives. *Adv. Funct. Mater.* **2009**, *19*, 772–778. DOI: [10.1002/adfm.200800829](https://doi.org/10.1002/adfm.200800829).
- [56] Mieno, H.; Yasuda, T.; Yang, Y. S.; Adachi, C. Self-Assembly, Physicochemical, and Field-Effect Transistor Properties of Solution-Crystallized Organic Semiconductors Based on π -Extended Dithieno[3,2-*b*:2',3'-*d*]Thiophenes. *Chem. Lett.* **2014**, *43*, 293–295. DOI: [10.1246/cl.130914](https://doi.org/10.1246/cl.130914).
- [57] Yang, Y.-S.; Yasuda, T.; Kakizoe, H.; Mieno, H.; Kino, H.; Tateyama, Y.; Adachi, C. High Performance Organic Field-Effect Transistors Based on Single-Crystal Microribbons and Microsheets of Solution-Processed Dithieno[3,2-*b*:2',3'-*d*]Thiophene Derivatives. *Chem. Commun.* **2013**, *49*, 6483–6485. DOI: [10.1039/c3cc42114g](https://doi.org/10.1039/c3cc42114g).
- [58] Yang, L.-P.; Wang, M.-M.; Slattum, P. M.; Bunes, B. R.; Wang, Y.-H.; Wang, C.-Y.; Zang, L. Donor-Acceptor Supramolecular Organic Nanofibers as Visible-Light

- Photoelectrocatalysts for Hydrogen Production. *ACS Appl. Mater. Interfaces* **2018**, *10*, 19764–19772. DOI: [10.1021/acsami.8b05637](https://doi.org/10.1021/acsami.8b05637).
- [59] Zang, L. Interfacial Donor-Acceptor Engineering of Nanofiber Materials to Achieve Photoconductivity and Applications. *Acc. Chem. Res.* **2015**, *48*, 2705–2714. DOI: [10.1021/acs.accounts.5b00176](https://doi.org/10.1021/acs.accounts.5b00176).
- [60] Lüttich, F.; Lehmann, D.; Friedrich, M.; Chen, Z.-H.; Facchetti, A.; Christian, V. B.; Zahn, R. T. D.; Harald, G. Interface Properties of OFETs Based on an Air-Stable n-Channel Perylene Tetracarboxylic Diimide Semiconductor. *Phys. Status Solidi A* **2012**, *209*, 585–593. DOI: [10.1002/pssa.201127592](https://doi.org/10.1002/pssa.201127592).
- [61] Wu, N.; Wang, C.; Bunes, B. R.; Zhang, Y.-Q.; Slattum, P. M.; Yang, X.-M.; Zang, L. Chemical Self-Doping of Organic Nanoribbons for High Conductivity and Potential Application as Chemiresistive Sensor. *ACS Appl. Mater. Interfaces* **2016**, *8*, 12360–12368. DOI: [10.1021/acsami.6b03151](https://doi.org/10.1021/acsami.6b03151).
- [62] Würthner, F. Perylene Bisimide Dyes as Versatile Building Blocks for Functional Supramolecular Architectures. *Chem. Commun.* **2004**, *14*, 1564–1579. DOI: [10.1039/B401630K](https://doi.org/10.1039/B401630K).
- [63] Kim, C.; Facchetti, A.; Marks, T. J. Gate Dielectric Microstructural Control of Pentacene Film Growth Mode and Field-Effect Transistor Performance. *Adv. Mater.* **2007**, *19*, 2561–2566. DOI: [10.1002/adma.200700101](https://doi.org/10.1002/adma.200700101).
- [64] Yoon, M.-H.; Kim, C.; Facchetti, A.; Marks, T. J. Gate Dielectric Chemical Structure-Organic Field-Effect Transistor Performance Correlations for Electron, Hole, and Ambipolar Organic Semiconductors. *J. Am. Chem. Soc.* **2006**, *128*, 12851–12869. DOI: [10.1021/ja063290d](https://doi.org/10.1021/ja063290d).
- [65] Chen, M.-C.; Kim, C.; Chen, S.-Y.; Chiang, Y.-J.; Chung, M.-C.; Facchetti, A.; Marks, T. J. Functionalized Anthradithiophenes for Organic Field-Effect Transistors. *J. Mater. Chem.* **2008**, *18*, 1029–1036. DOI: [10.1039/b715746k](https://doi.org/10.1039/b715746k).
- [66] Kwon, J.; Kim, T. M.; Oh, H.-S.; Kim, J.-J.; Hong, J.-I. Vacuum Processable Donor Material Based on Dithieno[3,2-*b*:2',3'-*d*]Thiophene and Pyrene for Efficient Organic Solar Cells. *RSC Adv.* **2014**, *4*, 24453–24457. DOI: [10.1039/C4RA02895C](https://doi.org/10.1039/C4RA02895C).
- [67] Ning, Z.-J.; Tian, H. Triarylamine: A Promising Core Unit for Efficient Photovoltaic Material. *Chem. Commun.* **2009**, *45*, 5483–5495. DOI: [10.1039/b908802d](https://doi.org/10.1039/b908802d).
- [68] Chen, C.; Yang, X.-C.; Cheng, M.; Zhang, F.-G.; Sun, L.-C. Degradation of Cyanoacrylic Acid-Based Organic Sensitizers in Dye-Sensitized Solar Cells. *ChemSusChem* **2013**, *6*, 1270–1275. DOI: [10.1002/cssc.201200949](https://doi.org/10.1002/cssc.201200949).
- [69] Sharma, G. D.; Mikroyannidis, J. A.; Roy, M. S.; Thomas, K. R. J.; Ball, R. J.; Kurchania, R. Dithienylthienothiadiazole-Based Organic Dye Containing Two Cyanoacrylic Acid Anchoring Units for Dye-Sensitized Solar Cells. *RSC Adv.* **2012**, *2*, 11457–11464. DOI: [10.1039/c2ra21718j](https://doi.org/10.1039/c2ra21718j).
- [70] Liu, X.-P.; Kong, F.-T.; Guo, F.-L.; Cheng, T.; Chen, W.-C.; Yu, T.; Chen, J.; Tan, Z.-A.; Dai, S.-Y. Influence of π -Linker on Triphenylamine-Based Hole Transporting Materials in Perovskite Solar Cells. *Dyes Pigments* **2017**, *139*, 129–135. DOI: [10.1016/j.dyepig.2016.12.022](https://doi.org/10.1016/j.dyepig.2016.12.022).
- [71] Ezhumalai, Y.; Lee, B.; Fan, M.-S.; Harutyunyan, B.; Prabakaran, K.; Lee, C.-P.; Chang, S. H.; Ni, J. S.; Vegiraju, S.; Priyanka, P.; et al. Metal-Free Branched Alkyl Tetrathienoacene (TTAR)-Based Sensitizers for High-Performance Dye-Sensitized Solar Cells. *J. Mater. Chem. A* **2017**, *5*, 12310–12321. DOI: [10.1039/C7TA01825H](https://doi.org/10.1039/C7TA01825H).
- [72] Zhou, N.-J.; Prabakaran, K.; Lee, B.; Chang, S. H.; Harutyunyan, B.; Guo, P.-J.; Butler, M. R.; Timalisina, A.; Bedzyk, M. J.; Ratner, M. A.; et al. Metal-Free Tetrathienoacene Sensitizers for High-Performance Dye-Sensitized Solar Cells. *J. Am. Chem. Soc.* **2015**, *137*, 4414–4423. DOI: [10.1021/ja513254z](https://doi.org/10.1021/ja513254z).
- [73] Deng, D.; Yang, Y.; Zhang, J.; He, C.; Zhang, M.-J.; Zhang, Z.-G.; Zhang, Z.-J.; Li, Y.-F. Triphenylamine-Containing Linear D-A-D Molecules with Benzothiadiazole as Acceptor Unit for Bulk-Heterojunction Organic Solar Cells. *Org. Electron* **2011**, *12*, 614–622. DOI: [10.1016/j.orgel.2011.01.013](https://doi.org/10.1016/j.orgel.2011.01.013).
- [74] Xiao, Z.-Y.; Sun, K.; Subbiah, J.; Ji, S.; Jones, D. J.; Wong, W. W. H. Hydrogen Bonding in Bulk Heterojunction Solar Cells: A Case Study. *Sci. Rep.* **2014**, *4*, 5701. DOI: [10.1038/srep05701](https://doi.org/10.1038/srep05701).

- [75] Lee, M.-W.; Kim, J.-Y.; Lee, D.-H.; Ko, M. J. Novel D- π -a Organic Dyes with Thieno[3,2-*b*]Thiophene-3,4-Ethylenedioxythiophene Unit as a π -Bridge for Highly Efficient Dye-Sensitized Solar Cells with Long-Term Stability. *ACS Appl. Mater. Interfaces* **2014**, *6*, 4102–4108. DOI: [10.1021/am405686z](https://doi.org/10.1021/am405686z).
- [76] Kim, J.; Shim, H.-S.; Lee, H.; Choi, M.-S.; Kim, J.-J.; Seo, Y. Highly Efficient Vacuum-Processed Organic Solar Cells Containing Thieno[3,2-*b*]Thiophene-Thiazole. *J. Phys. Chem. C* **2014**, *118*, 11559–11565. DOI: [10.1021/jp5017467](https://doi.org/10.1021/jp5017467).
- [77] Yang, J.-B.; Ganesan, P.; Teuscher, J.; Moehl, T.; Kim, Y. J.; Yi, C.-Y.; Comte, P.; Pei, K.; Holcombe, T. W.; Nazeeruddin, M. K.; et al. Influence of the Donor Size in D- π -a Organic Dyes for Dye-Sensitized Solar Cells. *J. Am. Chem. Soc.* **2014**, *136*, 5722–5730. DOI: [10.1021/ja500280r](https://doi.org/10.1021/ja500280r).
- [78] Zoombelt, A. P.; Mathijssen, S. G. J.; Turbiez, M. G. R.; Wienk, M. M.; Janssen, R. A. J. Small Band Gap Polymers Based on Diketopyrrolopyrrole. *J. Mater. Chem.* **2010**, *20*, 2240–2246. DOI: [10.1039/b919066j](https://doi.org/10.1039/b919066j).
- [79] Qu, S.-Y.; Tian, H. Diketopyrrolopyrrole (DPP)-Based Materials for Organic Photovoltaics. *Chem. Commun.* **2012**, *48*, 3039–3051. DOI: [10.1039/c2cc17886a](https://doi.org/10.1039/c2cc17886a).
- [80] Bijleveld, J. C.; Gevaerts, V. S.; Nuzzo, D. D.; Turbiez, M.; Mathijssen, S. G. J.; Leeuw, D. M. D.; Wienk, M. M.; Janssen, R. A. J. Efficient Solar Cells Based on an Easily Accessible Diketopyrrolopyrrole Polymer. *Adv. Mater.* **2010**, *22*, E242–E246. DOI: [10.1002/adma.201001449](https://doi.org/10.1002/adma.201001449).
- [81] Li, W.-W.; Hendriks, K. H.; Wienk, M. M.; Janssen, R. A. J. Diketopyrrolopyrrole Polymers for Organic Solar Cells. *Acc. Chem. Res.* **2016**, *49*, 78–85. DOI: [10.1021/acs.accounts.5b00334](https://doi.org/10.1021/acs.accounts.5b00334).
- [82] Zhou, N.-J.; Vegiraju, S.; Yu, X.-G.; Manley, E. F.; Butler, M. R.; Leonardi, M. J.; Guo, P.-J.; Zhao, W.; Hu, Y.; Prabakaran, K.; et al. Diketopyrrolopyrrole (DPP) Functionalized Tetrathienothiophene (TTA) Small Molecules for Organic Thin Film Transistors and Photovoltaic Cells. *J. Mater. Chem. C* **2015**, *3*, 8932–8941. DOI: [10.1039/C5TC01348H](https://doi.org/10.1039/C5TC01348H).
- [83] Lu, C.; Chen, W.-C. Diketopyrrolopyrrole-Thiophene-Based Acceptor-Donor-Acceptor Conjugated Materials for High-Performance Field-Effect Transistors. *Chem. Asian J.* **2013**, *8*, 2813–2821. DOI: [10.1002/asia.201300677](https://doi.org/10.1002/asia.201300677).
- [84] Wu, T.; Yu, C.-M.; Guo, Y.-L.; Liu, H.-T.; Yu, G.; Fang, Y.; Liu, Y.-Q. Synthesis, Structures, and Properties of Thieno[3,2-*b*]Thiophene and Dithiophene Bridged Isoindigo Derivatives and Their Organic Field-Effect Transistors Performance. *J. Phys. Chem. C* **2012**, *116*, 22655–22662. DOI: [10.1021/jp304697r](https://doi.org/10.1021/jp304697r).
- [85] Kim, C.; Chen, M.-C.; Chiang, Y.-J.; Guo, Y.-J.; Huang, H.; Liang, Y.-J.; Lin, Y.-J.; Huang, Y.-W.; Hu, T.-S.; et al. Functionalized Dithieno[2,3-*b*:3',2'-*d*]Thiophenes (DTTs) for Organic Thin-Film Transistors. *Org. Electron* **2010**, *11*, 801–813. DOI: [10.1016/j.orgel.2010.01.022](https://doi.org/10.1016/j.orgel.2010.01.022).
- [86] Youn, J.; Vegiraju, S.; Emery, J. D.; Leever, B. J.; Kewalramani, S.; Lou, S. J.; Zhang, S. M.; Prabakaran, K.; Ezhumalai, Y.; Kim, C.; et al. Diperfluorophenyl Fused Thiophene Semiconductors for n-Type Organic Thin Film Transistors (OTFTs). *Adv. Electron. Mater.* **2015**, *1*, 1500098. DOI: [10.1002/aelm.201500098](https://doi.org/10.1002/aelm.201500098).
- [87] Khan, Q. U.; Tian, G.-F.; Bao, L.; Qi, S.-L.; Wu, D. Z. Highly Uniform Supramolecular Nano-Films Derived from Carbazole-Containing Perylene Diimide via Surface-Supported Self-Assembly and Their Electrically Bistable Memory Behavior. *New J. Chem.* **2018**, *42*, 11506–11515. DOI: [10.1039/C8NJ01380B](https://doi.org/10.1039/C8NJ01380B).
- [88] Anthony, J. E. Functionalized Acenes and Heteroacenes for Organic Electronics. *Chem. Rev.* **2006**, *106*, 5028–5048. DOI: [10.1021/cr050966z](https://doi.org/10.1021/cr050966z).
- [89] Nam, S.; Jang, J.; Anthony, J. E.; Park, J.-J.; Park, C. E.; Kim, K. High-Performance Triethylsilylethynyl Anthradithiophene Transistors Prepared without Solvent Vapor Annealing: The Effects of Self-Assembly during Dip-Coating. *ACS Appl. Mater. Interfaces* **2013**, *5*, 2146–2154. DOI: [10.1021/am303192b](https://doi.org/10.1021/am303192b).
- [90] Li, R.-J.; Hu, W.-P.; Liu, Y.-Q.; Zhu, D.-B. Micro- and Nanocrystals of Organic Semiconductors. *Acc. Chem. Res.* **2010**, *43*, 529–540. DOI: [10.1021/ar900228v](https://doi.org/10.1021/ar900228v).

- [91] Moon, H.; Zeis, R.; Borkent, E.-J.; Besnard, C.; Lovinger, A. J.; Siegrist, T.; Kloc, C.; Bao, Z.-N. Synthesis, Crystal Structure, and Transistor Performance of Tetracene Derivatives. *J. Am. Chem. Soc.* **2004**, *126*, 15322–15323. DOI: [10.1021/ja045208p](https://doi.org/10.1021/ja045208p).
- [92] Ming, S.-L.; Zhen, S.-J.; Lin, K.-W.; Zhao, L.; Xu, J.-K.; Lu, B.-Y. Thiadiazolo[3,4-c]Pyridine as an Acceptor toward Fast-Switching Green Donor-Acceptor-Type Electrochromic Polymer with Low Bandgap. *ACS Appl. Mater. Interfaces* **2015**, *7*, 11089–11098. DOI: [10.1021/acsami.5b01188](https://doi.org/10.1021/acsami.5b01188).
- [93] Lu, B.-Y.; Zhen, S.-J.; Zhang, S.-M.; Xu, J.-K.; Zhao, G.-Q. Highly Stable Hybrid Selenophene-3,4-Ethylenedioxythiophene as Electrically Conducting and Electrochromic Polymers. *Polym. Chem.* **2014**, *5*, 4896–4908. DOI: [10.1039/C4PY00529E](https://doi.org/10.1039/C4PY00529E).
- [94] Lin, K.-W.; Chen, S.; Lu, B.-Y.; Xu, J.-K. Hybrid π -Conjugated Polymers from Dibenzopentacyclic Centers: Precursor Design, Electrosynthesis and Electrochromics. *Sci. China Chem.* **2017**, *60*, 38–53. DOI: [10.1007/s11426-016-0298-2](https://doi.org/10.1007/s11426-016-0298-2).
- [95] Yang, H.-Y.; Yen, Y.-S.; Hsu, Y.-C.; Chou, H.-H.; Lin, J. T. Organic Dyes Incorporating the Dithieno[3,2-*b*:2',3'-*d*]Thiophene Moiety for Efficient Dye-Sensitized Solar Cells. *Org. Lett.* **2010**, *12*, 16–19. DOI: [10.1021/ol902327p](https://doi.org/10.1021/ol902327p).
- [96] Cheng, Y.-J.; Yang, S.-H.; Hsu, C.-S. Synthesis of Conjugated Polymer for Organic Solar Cell Applications. *Chem. Rev.* **2009**, *109*, 5868–5923. DOI: [10.1021/cr900182s](https://doi.org/10.1021/cr900182s).
- [97] Biniek, L.; Fall, S.; Chochos, C. L.; Leclerc, N.; L  v  que, P.; Heiser, T. Optimization of the Side-Chain Density to Improve the Charge Transport and Photovoltaic Performances of a Low Band Gap Copolymer. *Org. Electron* **2012**, *13*, 114–120. DOI: [10.1016/j.orgel.2011.10.011](https://doi.org/10.1016/j.orgel.2011.10.011).
- [98] Patil, A. V.; Lee, W.-H.; Kim, K.; Lee, Y.-S.; Kang, I.-N.; Lee, S.-H. Synthesis and Characterization of Dithienothiophene/Benzothiadiazole Based Low Band Gap Donor-Acceptor Copolymers for Bulk Hetero Junction Photovoltaic Cells. *Synth. Met.* **2011**, *161*, 1838–1844. DOI: [10.1016/j.synthmet.2011.06.016](https://doi.org/10.1016/j.synthmet.2011.06.016).
- [99] Kini, G. P.; Lee, S. K.; Shin, W. S.; Moon, S.-J.; Song, C. E.; Lee, J.-C. Achieving a Solar Power Conversion Efficiency Exceeding 9% by Modifying the Structure of a Simple, Inexpensive and Highly Scalable Polymer. *J. Mater. Chem. A* **2016**, *4*, 18585–18597. DOI: [10.1039/C6TA08356K](https://doi.org/10.1039/C6TA08356K).
- [100] Jo, J. W.; Jung, J. W.; Ahn, H.; Ko, M. J.; Jen, A. K.-Y.; Son, H. J. Effect of Molecular Orientation of Donor Polymers on Charge Generation and Photovoltaic Properties in Bulk Heterojunction All-Polymer Solar Cells. *Adv. Energy Mater.* **2017**, *7*, 1601365. DOI: [10.1002/aenm.201601365](https://doi.org/10.1002/aenm.201601365).
- [101] Meager, I.; Ashraf, R.; S.; Mollinger, S.; Schroeder, B. C.; Bronstein, H.; Beatrup, D.; Vezie, M. S.; Kirchartz, T.; Salleo, A.; Nelson, J.; et al. Photocurrent Enhancement from Diketopyrrolopyrrole Polymer Solar Cells through Alkyl-Chain Branching Point Manipulation. *J. Am. Chem. Soc.* **2013**, *135*, 11537–11540. DOI: [10.1021/ja406934j](https://doi.org/10.1021/ja406934j).
- [102] Kim, K. H.; Chung, D. S.; Park, C. E.; Choi, D. H. π -Conjugated Main Chain Polymers Containing Bis(Bithiophenyl Dithienothiophene)-Based Repeating Group and Their Application to Polymer Solar Cells. *Mol. Cryst. Liq. Cryst.* **2011**, *538*, 187–192. DOI: [10.1080/15421406.2011.563720](https://doi.org/10.1080/15421406.2011.563720).
- [103] Choi, S.; Park, G. E.; Shin, J.; Um, H. A.; Cho, M. J.; Choi, D. H. Dithienothiophene-Diketopyrrolopyrrole-Containing Copolymers with Alkyl Side-Chain and Their Application to Polymer Solar Cells. *Synth. Met.* **2016**, *212*, 167–173. DOI: [10.1016/j.synthmet.2015.12.013](https://doi.org/10.1016/j.synthmet.2015.12.013).
- [104] Kong, R.; Xiao, Z.; Xie, F.-Y.; Jiang, J.-X.; Ding, L.-M. A D-A Copolymer Donor Containing an Alkylthio-Substituted Thieno[3,2-*b*]Thiophene Unit. *New J. Chem.* **2017**, *41*, 2895–2898. DOI: [10.1039/C6NJ03991J](https://doi.org/10.1039/C6NJ03991J).
- [105] Shahid, M.; Ashraf, R. S.; Huang, Z.-G.; Kronemeijer, A. J.; McCarthy-Ward, T.; McCulloch, I.; Durrant, J. R.; S  rri  nghaus, H. S.; Heeney, M. Photovoltaic and Field Effect Transistor Performance of Selenophene and Thiophene Diketopyrrolopyrrole Co-Polymers with Dithienothiophene. *J. Mater. Chem.* **2012**, *22*, 12817–12823. DOI: [10.1039/c2jm31189e](https://doi.org/10.1039/c2jm31189e).
- [106] Zeng, Z.; Li, Y.; Deng, J.-F.; Huang, Q.; Peng, Q. Synthesis and Photovoltaic Performance of Low Band Gap Copolymers Based on Diketopyrrolopyrrole and

- Tetrathienoacene with Different Conjugated Bridges. *J. Mater. Chem. A* **2014**, *2*, 653–662. DOI: [10.1039/C3TA14022A](https://doi.org/10.1039/C3TA14022A).
- [107] Li, Y.-X.; Lee, T. H.; Park, S. Y.; Uddin, M. A.; Kim, T.; Hwang, S.; Kim, J. Y.; Woo, H. Y. Straight Chain D-A Copolymers Based on Thienothiophene and Benzothiadiazole for Efficient Polymer Field Effect Transistors and Photovoltaic Cells. *Polym. Chem.* **2016**, *7*, 4638–4646. DOI: [10.1039/C6PY00674D](https://doi.org/10.1039/C6PY00674D).
- [108] Kim, J.-H.; Park, J. B.; Jung, I. H.; Grimsdale, A. C.; Yoon, S. C.; Yang, H.; Hwang, D.-H. Well-Controlled Thieno[3,4-c]Pyrrole-4,6-(5H)-Dione Based Conjugated Polymers for High Performance Organic Photovoltaic Cells with the Power Conversion Efficiency Exceeding 9%. *Energy Environ. Sci.* **2015**, *8*, 2352–2356. DOI: [10.1039/C5EE01627D](https://doi.org/10.1039/C5EE01627D).
- [109] Bronstein, H.; Chen, Z.-Y.; Ashraf, R. S.; Zhang, W.-M.; Du, J.-P.; Durrant, J. R.; Tuladhar, P. S.; Song, K.; Watkins, S. E.; Geerts, Y.; et al. Thieno[3,2-*b*] thiophene-Diketopyrrolopyrrole-Containing Polymers for High-Performance Organic Field-Effect Transistors and Organic Photovoltaic Devices. *J. Am. Chem. Soc.* **2011**, *133*, 3272–3275. DOI: [10.1021/ja110619k](https://doi.org/10.1021/ja110619k).
- [110] Lee, S. K.; Lee, J.; Lee, H. Y.; Yoon, S. C.; Kim, J. R.; Kim, K. N.; Kim, H. J.; Shin, W. S.; Moon, S.-J. Synthesis and Characterization of New Dithienosilole-Based Copolymers for Polymer Solar Cells. *J. Nanosci. Nanotechnol.* **2011**, *11*, 4279–4284. DOI: [10.1166/jnn.2011.3699](https://doi.org/10.1166/jnn.2011.3699).
- [111] Patil, A. V.; Lee, W.-H.; Lee, E.; Kim, K.; Kang, I.-N.; Lee, S.-H. Synthesis and Photovoltaic Properties of a Low-Band-Gap Copolymer of Dithieno[3,2-*b*:2',3'-*d*] Thiophene and Dithienylquinoxaline. *Macromolecules* **2011**, *44*, 1238–1241. DOI: [10.1021/ma102722d](https://doi.org/10.1021/ma102722d).
- [112] Zhang, X.-N.; Johnson, J. P.; Kampf, J. W.; Matzger, A. J. Ring Fusion Effects on the Solid-State Properties of Alpha-Oligothiophenes. *Chem. Mater.* **2006**, *18*, 3470–3476. DOI: [10.1021/cm0609348](https://doi.org/10.1021/cm0609348).
- [113] Yi, W.-J.; Zhao, S.; Sun, H.-L.; Kan, Y.-H.; Shi, J.-W.; Wan, S.-S.; Li, C.-L.; Wang, H. Isomers of Organic Semiconductors Based on Dithienothiophenes: The Effect of Sulphur Atoms Positions on the Intermolecular Interactions and Field-Effect Performances. *J. Mater. Chem. C* **2015**, *3*, 10856–10861. DOI: [10.1039/C5TC02287H](https://doi.org/10.1039/C5TC02287H).
- [114] Ding, Z.-Q.; Abbas, G.; Assender, H. E.; Morrison, J. J.; Yeates, S. G.; Patchett, E. R.; Taylor, D. M. Effect of Oxygen, Moisture and Illumination on the Stability and Reliability of Dinaphtho[2,3-*b*:2',3'-*f*]Thieno[3,2-*b*]Thiophene (DNFT) OTFTs during Operation and Storage. *ACS Appl. Mater. Interfaces* **2014**, *6*, 15224–15231. DOI: [10.1021/am503560d](https://doi.org/10.1021/am503560d).
- [115] Zhang, Y.-Y.; Ichikawa, M.; Hattori, J.; Kato, T.; Sazaki, A.; Kanazawa, S.; Kato, S.; Zhang, C.-H.; Taniguchi, Y. Fused Thiophene-Split Oligothiophenes with High Ionization Potentials for OTFTs. *Synth. Met.* **2009**, *159*, 1890–1895. DOI: [10.1016/j.synthmet.2009.06.016](https://doi.org/10.1016/j.synthmet.2009.06.016).
- [116] Cai, Z.-X.; Luo, H.-W.; Qi, P.-L.; Wang, J.-G.; Zhang, G.-X.; Liu, Z.-T.; Zhang, D.-P. Alternating Conjugated Electron Donor-Acceptor Polymers Entailing Pechmann Dye Framework as the Electron Acceptor Moieties for High Performance Organic Semiconductors with Tunable Characteristics. *Macromolecules* **2014**, *47*, 2899–2906. DOI: [10.1021/ma5003694](https://doi.org/10.1021/ma5003694).
- [117] Sun, B.; Hong, W.; Aziz, H.; Li, Y.-N. A Pyridine-Flanked Diketopyrrolopyrrole (DPP)-Based Donor-Acceptor Polymer Showing High Mobility in Ambipolar and n-Channel Organic Thin Film Transistors. *Polym. Chem.* **2015**, *6*, 938–945. DOI: [10.1039/C4PY01193G](https://doi.org/10.1039/C4PY01193G).
- [118] Park, G. E.; Shin, J.; Lee, D. H.; Lee, T. W.; Shim, H.; Cho, M. J.; Pyo, S.; Choi, D. H. Acene-Containing Donor-Acceptor Conjugated Polymers: Correlation between the Structure of Donor Moiety, Charge Carrier Mobility, and Charge Transport Dynamics in Electronic Devices. *Macromolecules* **2014**, *47*, 3747–3754. DOI: [10.1021/ma500733y](https://doi.org/10.1021/ma500733y).
- [119] Jian, N.-N.; Gu, H.; Zhang, S.-M.; Liu, H.-T.; Qu, K.; Chen, S.; Liu, X.-M.; He, Y.-F.; Niu, G.-F.; Tai, S.-Y.; et al. Synthesis and Electrochromic Performances of Donor-Acceptor-Type Polymers from Chalcogenodiazolo [3,4-*c*]Pyridine and Alkyl ProDOTs. *Electrochim. Acta* **2018**, *266*, 263–275. DOI: [10.1016/j.electacta.2018.01.099](https://doi.org/10.1016/j.electacta.2018.01.099).

- [120] Zhang, W.-N.; Zhang, W.-W.; Liu, H.-T.; Jian, N.-N.; Qu, K.; Chen, S.; Xu, J.-K. O/W Microemulsion as Electrolyte for Electro-Polymerization of 3,4-Ethylenedioxythiophene. *J. Electroanal. Chem.* **2018**, *813*, 109–115. DOI: [10.1016/j.jelechem.2018.02.006](https://doi.org/10.1016/j.jelechem.2018.02.006).
- [121] Shao, S.; Shi, J.-J.; Murtaza, I.; Xu, P.-P.; He, Y.-W.; Ghosh, S.; Zhu, X.-S.; Perepichka, I. F.; Meng, H. Exploring the Electrochromic Properties of Poly(Thieno [3,2-*b*]Thiophene)s Decorated with Electron-Deficient Side Groups. *Polym. Chem.* **2017**, *8*, 769–784. DOI: [10.1039/C6PY01847E](https://doi.org/10.1039/C6PY01847E).
- [122] Shi, J.-J.; Zhu, X.-S.; Xu, P.-P.; Zhu, M.-M.; Guo, Y.-T.; He, Y.-W.; Hu, Z.; Murtaza, I.; Yu, H.-T.; Yan, L.-J.; et al. A Redox-Dependent Electrochromic Material: Tetri-EDOT Substituted Thieno[3,2-*b*]Thiophene. *Macromol. Rapid Commun.* **2016**, *37*, 1344–1351. DOI: [10.1002/marc.201600157](https://doi.org/10.1002/marc.201600157).
- [123] Xu, P.-P.; Murtaza, I.; Shi, J.-J.; Zhu, M.-M.; He, Y.-W.; Yu, H.-T.; Goto, O.; Meng, H. Highly Transmissive Blue Electrochromic Polymers Based on Thieno[3,2-*b*]Thiophene. *Polym. Chem.* **2016**, *7*, 5351–5356. DOI: [10.1039/C6PY00989A](https://doi.org/10.1039/C6PY00989A).
- [124] Zhu, X.-S.; Zhu, Y.-N.; Murtaza, I.; Shi, J.-J.; He, Y.-W.; Xu, P.-P.; Zhu, M.-M.; Goto, O.; Meng, H. Thieno[3,2-*b*]Thiophene Based Electrochromic Polymers: Experimental Cum Theoretical Appraisal of the EDOT Position. *RSC Adv.* **2016**, *6*, 75522–75529. DOI: [10.1039/C6RA12319H](https://doi.org/10.1039/C6RA12319H).
- [125] Akbaşoğlu, N.; Balan, A.; Baran, D.; Cirpan, A.; Toppare, L. Electrochemical and Optical Studies of Furan and Thieno[3,2-*b*]Thiophene End Capped Benzotriazole Derivatives. *J. Polym. Sci. A Polym. Chem.* **2010**, *48*, 5603–5610. DOI: [10.1002/pola.24375](https://doi.org/10.1002/pola.24375).
- [126] Granqvist, C. G.; Arvizu, M. A.; Pehlivan, I. B.; Qu, H.-Y.; Wen, R.-T.; Niklasson, G. A. Electrochromic Materials and Devices for Energy Efficiency and Human Comfort in Buildings: A Critical Review. *Electrochim. Acta* **2018**, *259*, 1170–1182. DOI: [10.1016/j.electacta.2017.11.169](https://doi.org/10.1016/j.electacta.2017.11.169).
- [127] Sahin, O.; Osken, I.; Ozturk, T. Investigation of Electrochromic Properties of Poly(3,5-Bis(4-Methoxyphenyl)Dithieno[3,2-*b*;2',3'-*d*]Thiophene). *Synth. Met.* **2011**, *161*, 183–187. DOI: [10.1016/j.synthmet.2010.11.020](https://doi.org/10.1016/j.synthmet.2010.11.020).
- [128] Cho, C. M.; Ye, Q.; Neo, W. T.; Lin, T.-T.; Lu, X.-H.; Xu, J.-W. Ultrahigh Electron-Deficient Pyrrolo-Acenaphtho-Pyridazine-Dione Based Donor-Acceptor Conjugated Polymers for Electrochromic Applications. *Polym. Chem.* **2015**, *6*, 7570–7579. DOI: [10.1039/C5PY01129A](https://doi.org/10.1039/C5PY01129A).
- [129] Li, W.-S.; Guo, Y.-T.; Shi, J.-J.; Yu, H.-T.; Meng, H. Solution-Processable Neutral Green Electrochromic Polymer Containing Thieno[3,2-*b*]Thiophene Derivative as Unconventional Donor Units. *Macromolecules* **2016**, *49*, 7211–7219. DOI: [10.1021/acs.macromol.6b01624](https://doi.org/10.1021/acs.macromol.6b01624).
- [130] Xue, Y.; Xue, Z.-X.; Zhang, W.-W.; Zhang, W.-N.; Chen, S.; Lin, K.-W.; Xu, J.-K. Effects on Optoelectronic Performances of EDOT End-Capped Oligomers and Electrochromic Polymers by Varying Thienothiophene Cores. *J. Electroanal. Chem.* **2019**, *834*, 150–160. DOI: [10.1016/j.jelechem.2019.01.007](https://doi.org/10.1016/j.jelechem.2019.01.007).
- [131] Xue, Y.; Xue, Z.-X.; Zhang, W.-W.; Zhang, W.-N.; Chen, S.; Lin, K.-W.; Xu, J.-K. Thieno[3,2-*b*]Thiophene End-Capped All-Sulfur Analog of 3,4-Ethylenedioxythiophene and Its Electrosynthesized Polymer: Is Distorted Conformation Not Suitable for Electrochromism? *J. Polym. Sci. Part A: Polym. Chem.* **2019**, *57*, 1041–1048. DOI: [10.1002/pola.29339](https://doi.org/10.1002/pola.29339).
- [132] Yuk, H.; Lu, B.-Y.; Zhao, X.-H. Hydrogel Bioelectronics. *Chem. Soc. Rev.* **2019**, *48*, 1642–1667. DOI: [10.1039/C8CS00595H](https://doi.org/10.1039/C8CS00595H).
- [133] Yersin, H.; Mataranga-Popa, L.; Li, S.-W.; Czerwieńiec, R. Design Strategies for Materials Showing Thermally Activated Delayed Fluorescence and beyond: Towards the Fourth-Generation OLED Mechanism. *J. Soc. Inf. Display* **2018**, *26*, 194–199. DOI: [10.1002/jsid.654](https://doi.org/10.1002/jsid.654).
- [134] Lim, E.; Jung, B.-J.; Shim, H.-K. Improved EL Efficiency of Fluorene-Thieno [3,2-*b*]Thiophene-Based Conjugated Copolymers with Hole-Transporting or Electron-

- Transporting Units in the Main Chain. *J. Polym. Sci. Part A: Polym. Chem.* **2006**, *44*, 243–253. DOI: [10.1002/pola.21144](https://doi.org/10.1002/pola.21144).
- [135] Bharti, M.; Singh, A.; Samanta, S.; Aswal, D. K. Conductive Polymers for Thermoelectric Power Generation. *Prog. Mater. Sci.* **2018**, *93*, 270–310. DOI: [10.1016/j.pmatsci.2017.09.004](https://doi.org/10.1016/j.pmatsci.2017.09.004).
- [136] DiSalvo, F. J. Thermoelectric Cooling and Power Generation. *Science* **1999**, *285*, 703–706. DOI: [10.1126/science.285.5428.703](https://doi.org/10.1126/science.285.5428.703).
- [137] Hochbaum, A. I.; Chen, R.; Delgado, R. D.; Liang, W.-J.; Garnett, E. C.; Najarian, M.; Majumdar, A.; Yang, P.-D. Enhanced Thermoelectric Performance of Rough Silicon Nanowires. *Nature* **2008**, *451*, 163–167. DOI: [10.1038/nature06381](https://doi.org/10.1038/nature06381).
- [138] Jiang, F.-X.; Xu, J.-K.; Lu, B.-Y.; Xie, Y.; Huang, R.-J.; Li, L.-F. Thermoelectric Performance of Poly(3,4-Ethylenedioxythiophene): Poly(Styrenesulfonate). *Chin. Phys. Lett.* **2008**, *25*, 2202–2205. DOI: [10.1088/0256-307x/25/6/076](https://doi.org/10.1088/0256-307x/25/6/076).
- [139] Shi, H.; Liu, C.-C.; Jiang, Q.-L.; Xu, J.-K. Effective Approaches to Improve the Electrical Conductivity of PEDOT:PSS: A Review. *Adv. Electron. Mater.* **2015**, *1*, 1500017. DOI: [10.1002/aelm.201500017](https://doi.org/10.1002/aelm.201500017).
- [140] Zhao, W.-Y.; Liu, Z.-Y.; Sun, Z.-G.; Zhang, Q.-J.; Wei, P.; Mu, X.; Zhou, H.-Y.; Li, C.-C.; Ma, S.-F.; He, D.-Q.; et al. Superparamagnetic Enhancement of Thermoelectric Performance. *Nature* **2017**, *549*, 247–251. DOI: [10.1038/nature23667](https://doi.org/10.1038/nature23667).
- [141] Yue, R.-R.; Chen, S.; Lu, B.-Y.; Liu, C.-C.; Xu, J.-K. Facile Electrosynthesis and Thermoelectric Performance of Electroactive Free-Standing Polythieno[3,2-*b*]Thiophene Films. *J. Solid State Electrochem.* **2011**, *15*, 539–548. DOI: [10.1007/s10008-010-1095-8](https://doi.org/10.1007/s10008-010-1095-8).
- [142] Yue, R.-R.; Chen, S.; Liu, C.-C.; Lu, B.-Y.; Xu, J.-K.; Wang, J.-M.; Liu, G.-D. Synthesis, Characterization, and Thermoelectric Properties of a Conducting Copolymer of 1,12-Bis(Carbazolyl)Dodecane and Thieno[3,2-*b*]Thiophene. *J. Solid State Electrochem.* **2012**, *16*, 117–126. DOI: [10.1007/s10008-011-1292-0](https://doi.org/10.1007/s10008-011-1292-0).
- [143] Zhou, W.-Q.; Xu, J.-K. Progress in Conjugated Polyindoles: Synthesis, Polymerization Mechanisms, Properties, and Applications. *Polym. Rev.* **2017**, *57*, 248–275. DOI: [10.1080/15583724.2016.1223130](https://doi.org/10.1080/15583724.2016.1223130).
- [144] Miller, J. R.; Simon, P. Electrochemical Capacitors for Energy Management. *Science* **2008**, *321*, 651–652. DOI: [10.1126/science.1158736](https://doi.org/10.1126/science.1158736).
- [145] El-Kady, M. F.; Strong, V.; Dubin, S.; Kaner, R. B. Laser Scribing of High-Performance and Flexible Graphene-Based Electrochemical Capacitors. *Science* **2012**, *335*, 1326–1330. DOI: [10.1126/science.1216744](https://doi.org/10.1126/science.1216744).
- [146] Ates, M.; Eren, N.; Osken, I.; Baslilar, S.; Ozturk, T. Poly(2,6-di(Thiophene-2-yl)-3,5-bis(4-(Thiophene-2-yl)Phenyl)Dithieno[3,2-*b*;2',3'-*d*]Thiophene)/Carbon Nanotube Composite for Capacitor Applications. *J. Appl. Polym. Sci.* **2014**, *131*, 40061–40069. DOI: [10.1002/app.40061](https://doi.org/10.1002/app.40061).
- [147] Dubal, D. P.; Ayyad, O.; Ruiz, V.; Gómez-Romero, P. Hybrid Energy Storage: The Merging of Battery and Supercapacitor Chemistries. *Chem. Soc. Rev.* **2015**, *44*, 1777–1790. DOI: [10.1039/C4CS00266K](https://doi.org/10.1039/C4CS00266K).
- [148] Zhou, W.-Q.; Du, Y.-K.; Ren, F.-F.; Wang, C.-Y.; Xu, J.-K.; Yang, P. High Efficient Electrocatalytic Oxidation of Methanol on Pt/Polyindoles Composite Catalysts. *Int. J. Hydrogen Energy* **2010**, *35*, 3270–3279. DOI: [10.1016/j.ijhydene.2010.01.083](https://doi.org/10.1016/j.ijhydene.2010.01.083).
- [149] Liang, A.; Li, D.; Zhou, W.; Wu, Y.; Ye, G.; Wu, J.; Chang, Y.; Wang, R.; Xu, J.; Nie, G.; et al. Robust Flexible WS₂/PEDOT:PSS Film for Use in High-Performance Miniature Supercapacitors. *J. Electroanal. Chem.* **2018**, *824*, 136–146. DOI: [10.1016/j.jelechem.2018.07.040](https://doi.org/10.1016/j.jelechem.2018.07.040).
- [150] Yamashita, Y.; Tsurumi, J.; Ohno, M.; Fujimoto, R.; Kumagai, S.; Kurosawa, T.; Okamoto, T.; Takeya, J.; Watanabe, S. Efficient Molecular Doping of Polymeric Semiconductors Driven by Anion Exchange. *Nature* **2019**, *572*, 634–638. DOI: [10.1038/s41586-019-1504-9](https://doi.org/10.1038/s41586-019-1504-9).